Doctoral Dissertation

Synthesis and properties of self-doped conducting polyanilines bearing phosphonic acid and phosphonic acid monoester

Yasushi Abe

December 2014

Daihachi Chemical Industry Co., Ltd.

Doctoral Dissertation

Synthesis and properties of self-doped conducting polyanilines bearing phosphonic acid and phosphonic acid monoester

(ホスホン酸およびホスホン酸モノエステルを有する自己ドープ型導電性ポリアニリンの合成と特性**)**

Yasushi Abe

December 2014

Daihachi Chemical Industry Co., Ltd.

Preface

The author dedicates this thesis to Mr. Yasuhiro Onishi.

The studies presented in this thesis are part of results as a collaborative project performed by Professor Dr. Toshikazu Hirao, Department of Applied Chemistry, Graduate School of Engineering, Osaka University and Daihachi Chemical Industry during 2012-2015. They were conducted under his guidance.

The objects of this thesis are the development of self-doped conducting polyanilines bearing phosphonic acid and phosphonic acid monoester.

The author hopes that the self-doped conducting polyanilines described in this thesis contribute to the further development for chemistry of self-doped conducting polymers.

Yasushi Abe

Osaka R&D Laboratory,
Daihachi Chemical Industry Co., Ltd.,
Higashiosaka, Osaka
Japan

December, 2014

Contents

General Introduction

Conducting polymers were first reported by Heeger, MacDiarmid, and Shirakawa in 1977,[1] and have since been widely researched and developed. Today, these polymers are used as conducting films and organic solar cell materials, among other applications, and play an important role in industry.[2]

The low stability of polyacetylenes has been one of the major impediments to the widespread application of conducting polymers, thereby prompting the development of the more stable polyanilines, polythiophenes, and polypyrrols as alternatives.[3] At the same time, alkyl chains and acidic functional groups have been introduced to conductive polymers to improve solubility and processability.[4] Fortunately, acidic functionalities not only improve solubility, but allow the resulting material to be self-doping as well, as first demonstrated by the sulfonated polyaniline reported by Epstein et al. in 1990.[5] This initial discovery in turn led to the development of a series of carbonated, phosphonated, and boronated analgos.[6]

However, despite the development of these newer classes of polyanilines, the majority of research and development has been restricted to sulfonated polyanilines, given the number of practically useful materials produced. For example, poly(2-methoxyaniline-5-sulfonic acid) (PMAS)[6k] (Figure 1) is marketed by Mitsubishi Rayon as a water-soluble conducting film with charge dissipation properties. However, the sulfonic acid moiety is strongly acidic and may not be appropriate for applications that involve basic materials. Therefore, it will be necessary to develop new self-doped polyanilines if such materials are to be more widely applied.

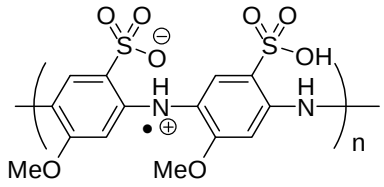

Figure 1. Structure of poly(2-methoxyaniline-5-sulfonic acid) (PMAS).

Polyanilines take on various oxidation states that can be structurally described as leucoemeraldine, emeraldine, and pernigraniline bases; protonated forms of the emeraldine base, referred to as emeraldine salts, also exist (Scheme 1). Out of all of these structures, it is the emeraldine salt that exhibits conductivity. However, these salts can take on two possible forms, with the extended coil exhibiting higher conductivity than the compact coil conformation. As such, conformational control is an important design concern.[7] Some progress has already been made in this regard; for example, Hirao and co-workers have reported that partial oxidation and reduction allows for the reversible control of PMAS conformation.[8]

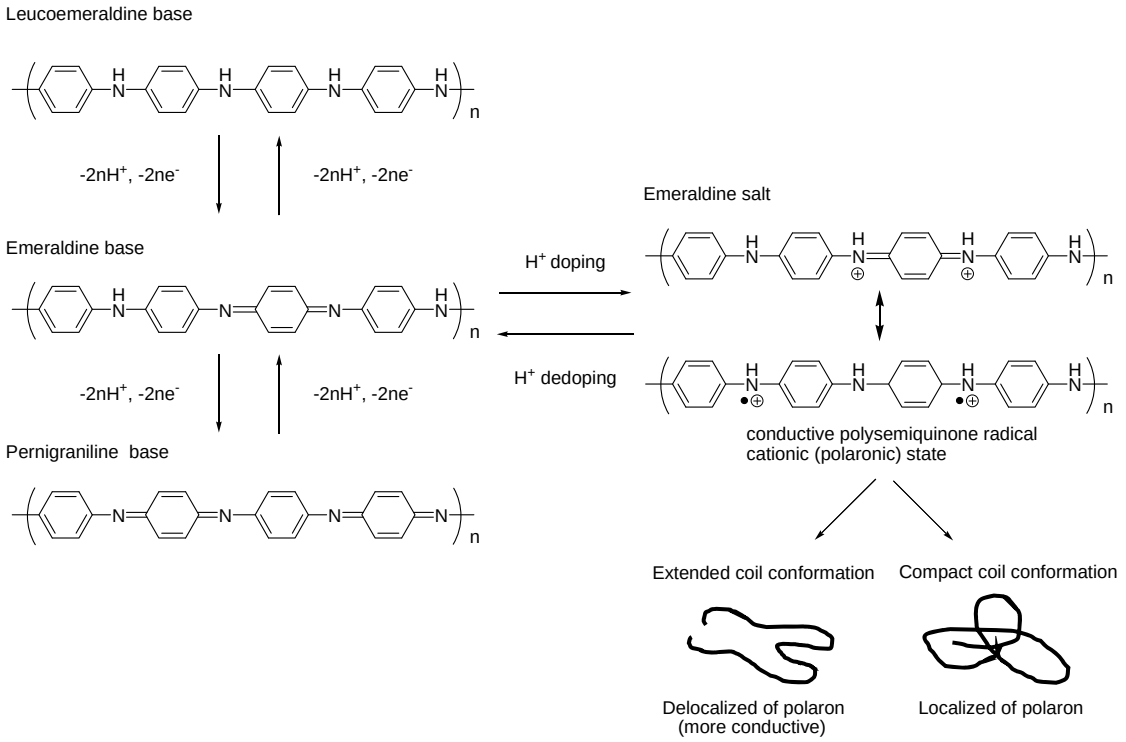

Scheme 1. Redox and conformation of polyaniline.

They have also reported that the PMAS used in hybrid catalysts with gold nanoparticles can act as a redox mediator for oxygen-based oxidation reactions.[9] In this context, the author designed two new self-doped conducting polyanilines that replace the sulfonic acid moiety of PMAS with either phosphonic acid or phosphic acid monoester, yielding poly(2-methoxyaniline-5-phosphonic acid) (PMAP) and poly(2-methoxyaniline-5-phosphonic acid monoethyl ester (PMAPE), respectively (Figure 2). Replacement with phosphonic acid was particularly attractive given that, like sulfonic acid, it is both sufficiently acidic to effect doping and functional moiety can be introduced to uninvolved acidic via covalent bonds or complexations. Chan et al.[10] have already reported the synthesis of polyaniline containing a phosphonic acid moiety, yet used a methylene unit to bridge the functional unit to the backbone (Figure 3); to be the best of the author's knowledge, there are no previous reports which demonstrate a direct link. Moreover, the synthesis of both diprotic PMAP and monoprotic PMAPE was completed in order to better elucidate the structure-property relationship of the acid moiety to the backbone. Once the polymers were successfully synthesized, their general properties were characterized and their charge dissipation properties were evaluated for their application as water-soluble conducting films in electron beam lithography.

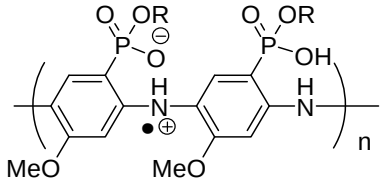

Poly(2-methoxyaniline-5-phosphonic acid) (PMAP) : R = H
Poly(2-methoxyaniline-5-phosphonic acid monoethyl ester) (PMAPE) : R = Et

Figure 2. Structures of PMAP and PMAPE.

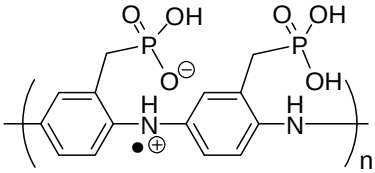

Figure 3. Structure of poly(*o*-aminobenzylphosphonic acid)

Chapter 1 describes an initial PMAP synthesis, while chapter 2 explores a more practical method. Chapter 3 then expands on this work, giving the synthesis for PMAPE. Chapter 4 reviews the properties of the synthesized polymers, with a focus on chemical oxidation and reduction. Meanwhile, chapter 5 investigates the pH dependence of polaron delocalization in aqueous solution. Finally, chapter 6 addresses practical applications, evaluating the charge dissipation of the PMAP/amine complex in electron beam lithography.

References and notes

1. H. Shirakawa, E. J. Louis, A. G. MacDiarmid, C. K. Chiang, A. J. Heeger, *J. Chem. Soc., Chem. Comm.* **1977**, 578-580.
2. (a) J. S. Miller, *Adv. Mater.* **1993**, *5*, 671-676. (b) M. Ates, T. Karazehir, A. S. Sarac, *Curr. Phys. Chem.* **2012**, *2*, 224-240.
3. S. Bhadra, D. Khastgir, N. K. Singha, J. H. Lee, *Prog. Polym. Sci.* **2009**, *34*, 783-810.
4. M. S. Freund, B. Deore, Self-doped Conducting Polymers, John Wiley & Sons Ltd., New York, 2007.
5. J. Yue, A. J. Epstein, *J. Am. Chem. Soc.* **1990**, *112*, 2800-2801.
6. (a) P. Hany, E. M. Geniès, C. Santier, *Synth. Met.* **1989**, *31*, 369-378. (b) J. Yue, A. J. Epstein, *J. Am. Chem. Soc.* **1990**, *112*, 2800-2801. (c) J.-Y. Bergeron, J.-W. Chevalier, L. H. Dao, *J. Chem. Soc. Chem. Commun.* **1990**, 180-181. (d) J. Yue, G. Gordon, A. J. Epstein, *Polymer* **1992**, *33*, 4410-4418. (e) H. S. O. Chan, S. C. Ng, A. S. Sim, K. L. Tan, B. T. G. Tan, *Macromolecules* **1992**, *25*, 6029-6034. (f) C. DeArmitt, S. P. Armes, J. Winter, F. A. Uribe, S. Gottesfeld, C.

Mombourquette, *Polymer* **1993**, *34*, 158-162. (g) M. T. Nguyen, P. Kasai, J. L. Miller, A. F. Diaz, *Macromolecules* **1994**, *27*, 3625-3631. (h) S. C. Ng, H. S. O. Chan, H. H. Huang, P. K. H. Ho, *J. Chem. Soc. Chem. Commun.* **1995**, 1327-1328. (i) H. S. O. Chan, P. K. H. Ho, S. C. Ng, B. T. G. Tan, K. L. Tan, *J. Am. Chem. Soc.* **1995**, *117*, 8517-8523. (j) X.-L. Wei, Y. Z. Wang, S. M. Long, C. Bobeczko, A. J. Epstein, *J. Am. Chem. Soc.* **1996**, *118*, 2545-2555. (k) S. Shimizu, T. Saitoh, M. Uzawa, M. Yuasa, K. Yano, T. Maruyama, K. Watanabe, Synth. Met. **1997**, *85*, 1337-1338. (l) M. Nicolas, B. Fabre, G. Marchand, J. Simonet, *Eur. J. Org. Chem.* **2000**, 1703-1710. (m) E. Shoji, M. S. Freund, *J. Am. Chem. Soc.* **2001**, *123*, 3383-3384. (n) N. Ohno, H.-J. Wang, H. Yan, N. Toshima, *Polym. J.* **2001**, *33*, 165-171. (o) C.-C.-C. Han, H. Lu, S.-P. Hong, K.-F. Yang, *Macromolecules* **2003**, *36*, 7908-7915. (p) A. Malinauskas, *J. Power Sources* **2004**, *126*, 214-220. (q) L.-J. Ghil, T.-Y. Youn, N.-R. Park, H.-W. Rhee, *J. Nanosci. Nanotechnol.* **2013**, *13*, 7912-7915.

7. (a) Y. Pornputtkul, E. V. Strounina, L. A. P. Kane-Maguire, G. G. Wallace, *Macromolecules* **2010**, *43*, 9982-9989. (b) E. V. Strounina, R. Shepherd, L. A. P. Kane-Maguire, G. G. Wallace, *Synth. Met.* **2003**, *135-136*, 289-290.
8. T. Amaya, D. Saio, S. Koga, T. Hirao, *Macromolecules* **2010**, *43*, 1175-1177.
9. D. Saio, T. Amaya, T. Hirao, *Adv. Synth. Catal.* **2010**, *352*, 2177-2182.
10. (a) S. C. Ng, H. S. O. Chan, H. H. Huang, P. K. H. Ho, *J. Chem. Soc. Chem. Commun.* **1995**, 1327-1328. (b) H. S. O. Chan, P. K. H. Ho, S. C. Ng, B. T. G. Tan, K. L. Tan, *J. Am. Chem. Soc.* **1995**, *117*, 8517-8523.

Chapter 1. PMAP Synthesis[P1]

1-1. Introduction

Organic conducting polymers containing covalently bound, charged functional groups that impact polymer properties are referred to as self-doped conducting polymers.[1] This definition includes polymers with acid groups covalently attached to the main chain, as they do not require an external dopant.

The integration of acid groups to polyaniline is generally accomplished either by direct modification of polyaniline or through the polymerization of an aniline monomer bearing the acid group. The latter allows for more flexibility in polymer design, and so was selected to synthesize the initial targets, poly(anilinephosphonic acid) (PAP) and PMAP (Figure 1).

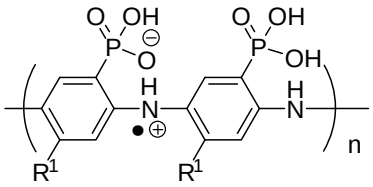

Poly(aniline-5-phosphonic acid) (PAP) : R^1 = H
Poly(2-methoxyaniline-5-phosphonic acid) (PMAP) : R^1 = OMe

Figure 1. Structures of PAP and PMAP.

Two acidic protons are available in phosphonic acids, allowing for additional acid/base complexation. In addition, previous reports suggest that alkylphosphonic acids are sufficiently acidic to dope the emeraldine base form of polyaniline.[2] Note that polyaniline self-doped with a phosphonic acid moiety attached directly to the backbone through a methylene chain has been previously synthesized;[3a,b] however, our design, which attaches the acid group directly to the backbone, is expected to exhibit more efficient self-doping because of its structure. Given all of this information, it was reasonable to conclude that the resulting polymer would show interesting and useful properties.

1-2. Results and discussion

The synthesis of PAP was attempted through oxidative polymerization of the aniline monomers **1a**[4a] or **1b**[4b] by using $(NH_4)_2S_2O_8$ as the oxidant (Scheme 1a). However, conducting polymers were not obtained in either case despite multiple attempts at changing the reaction conditions.

As a replacement, monomer **5**, a methoxy-substituted analog of **1a**, was designed with the intent of improving polymerization reactivity. As shown in Scheme 1b, a Pd-catalyzed coupling reaction

developed by Hirao and co-workers was employed to introduce the phosphonate group[5] to the commercially available bromonitroanisole **2**, using $HPO(OEt)_2$ in the presence of $Pd(OAc)_2$ (10 mol%) and Na_2CO_3 to afford the diethylphosphonate **3** in 69% yield. Hydrogenation of the nitro group, followed by acid-catalyzed hydrolysis, gave the aniline monomer **5** (2 steps, 72% yield). The obtained monomer **4** was then polymerized with $(NH_4)_2S_2O_8$ in 2.5 M aqueous pyridine solution at -5 °C for 5 d. Finally, the reaction mixture was treated with 1 M aqueous HCl solution; the desired polymer was obtained in 53% yield as a hard black solid.

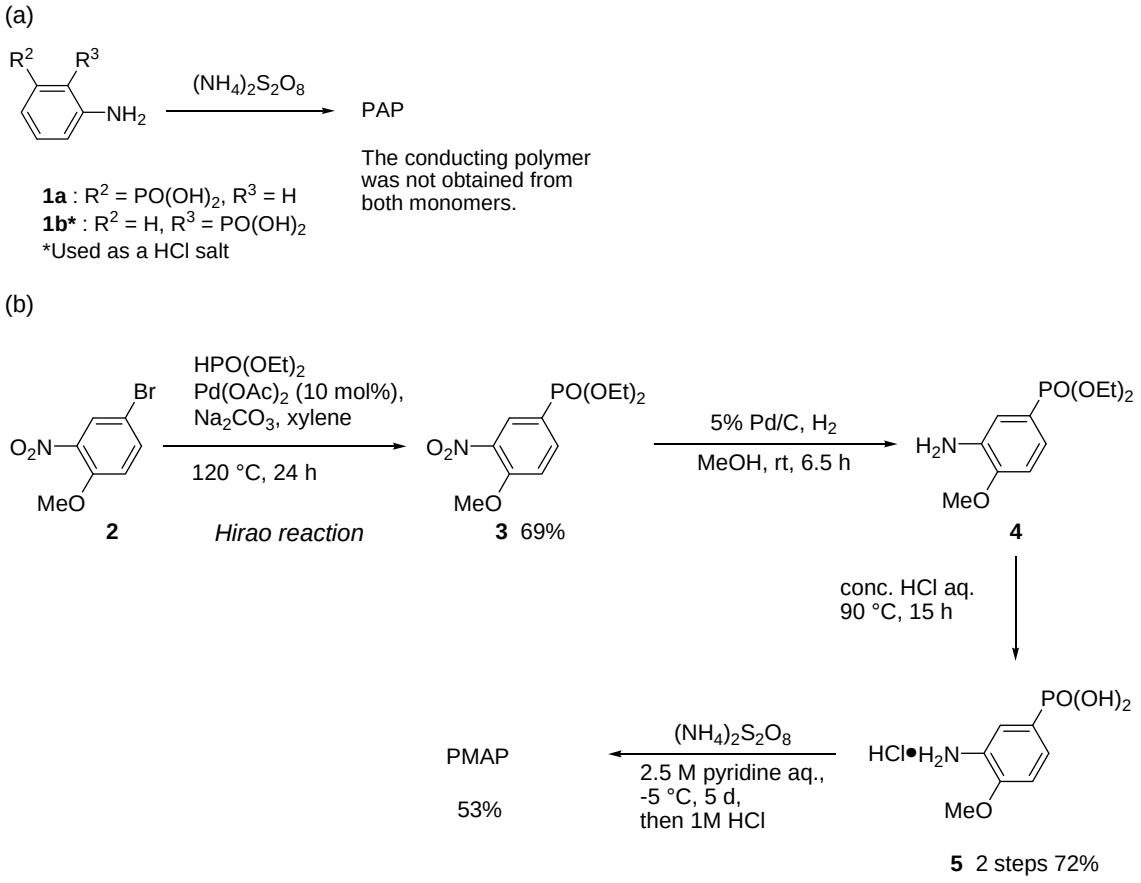

Scheme 1. (a) Polymerization of **1**. (b) Synthesis of monomer **5** and PMAP.

The obtained PMAP had a weight average molecular weight (*Mw*) of 2.0 x 10^3 and a polydispersity index of 2.7, as determined by gel permeation chromatography (GPC). Although the produced polymer did not show good solubility in acidic or neutral aqueous solution, it was soluble in basic aqueous media. The pyridinium salt, however, was soluble in neutral water as well.

Figure 2 shows the UV-vis-NIR spectrum of the obtained PMAP. The brown aqueous solution of the PMAP/pyridine complex (in a 1:1 molar ratio with respect to the aniline unit) formed at a pH of 5.35 was analyzed first. The polymer showed a maximum absorption at 281 nm, while the shoulder

peak at about 420 nm can be assigned as a polaron band. Steadily increasing absorption starting at about 1000 nm was also observed; this free carrier tail is highly characteristic of doped conducting polyanilines.[6]

On the other hand, a similar solution at a pH of 8.98 had maximum absorptions at 283 and 683 nm, and a shoulder peak at around 430 nm. Notably, the free carrier tail was observed in this case as well.

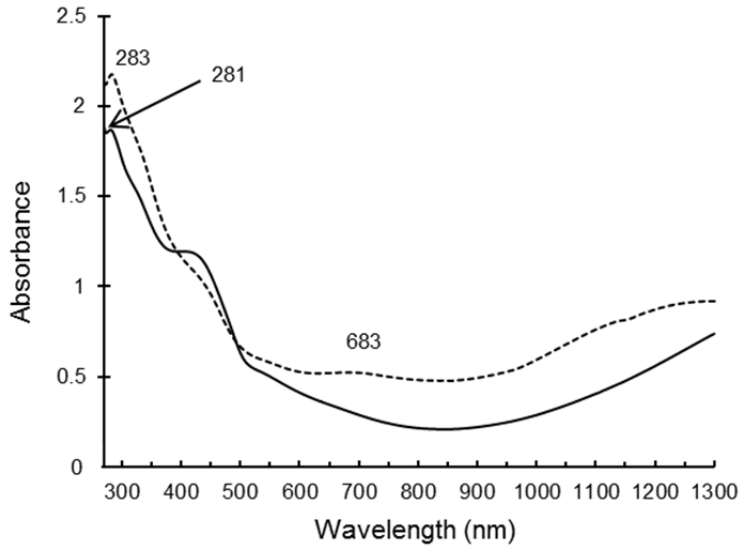

Figure 2. UV-vis-NIR spectra for PMAP at 298 K (4.9 x 10^{-4} M based on the aniline unit): PMAP/pyridine (1:1) in H_2O (pH 5.35) (solid line) and in the pH 8.98 aqueous solution (dashed line).

An aqueous solution of the PMAP/pyridine complex, this time at a molar ratio of 1:2 with respect to the aniline unit, was then assessed by electron spin resonance (ESR). The material exhibited a single resonance line centered at around g = 2.0036 without hyperfine coupling (Figure 3). This peak is characteristic of the delocalized free radicals that are to be expected in conducting polyaniline.[7]

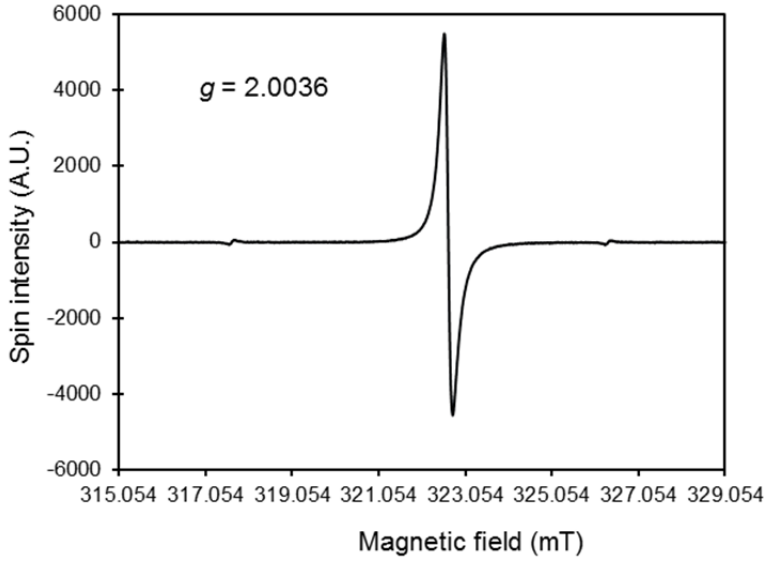

Figure 3. ESR spectrum for PMAP/pyridine (1:2) in H_2O at 298 K (4.9×10^{-2} M based on the aniline unit).

The electrical resistance of the polymer was measured by a direct-current (DC) method (Table 1). The tested films were formed by drop-casting an aqueous 1% (w/w) suspension or solution of the pyridinium salt on a glass substrate, onto which was placed a pair of indium tin oxide (ITO) electrodes with a built-in gap (width: 200 μm, height: 150 nm; see Figure 5 in the Experimental). Various PMAP/pyridine ratios were tested; note that at least a 1:2 ratio with respect to the aniline unit was needed to completely dissolve the material in solution prior to spin-coating. The electrical resistance of the films ranged from 14 to 20 kΩ, which corresponded to conductivities of 0.19-0.13 S/cm (Table 1).

Table 1. Electrical resistance and conductivity for the drop-cast films of the aqueous 1% (w/w) suspension or solution of the pyridinium salts of PMAP.

Entry	Molar equivalents of pyridine[a]	Suspension or solution	Electrical resistance (kΩ)	Conductivity[b] (S/cm)
1	1	Suspension	14	0.19
2	2	Solution	20	0.13
3	4	Solution	20	0.13

[a] Based on the aniline unit.
[b] Conductivity was calculated on the assumption that the gap (see Figure 5 in the Experimental) was filled with the polymer. Therefore, the obtained values are the minimum value.

Sheet resistance was measured by a four-point probe method. The tested film was formed by

drop-casting an aqueous 2% (w/w) solution of the PMAP/pyridine complex (at a molar ratio of 1:2 with respect to the aniline unit) on a glass substrate; an overall value of 3.8 x 10^6 Ω/□ was obtained.

An identical solution to the one used above was then spin-coated on a glass substrate (26 x 26 mm) to allow for surface analysis. A photo of the transparent light-brown film is shown in Figure 4. The thickness was 18 nm, as determined by a surface profiler. Scanning electron microscopy (SEM) images are shown in Figure 7 in the Experimental, and demonstrated a uniformly formed surface.

Figure 4. Photo of the spin-coating film formed with the aqueous 2% (w/w) solution of the pyridinium salt of PMAP (molar ratio = 1:2 based on the aniline unit) on a glass substrate (26 x 26 mm) and its thickness.

In conclusion, the self-doped conducting polyaniline PMAP was successfully synthesized via oxidative polymerization. This is the first example of a polyaniline bearing a phosphonic acid moiety attached directly to the backbone. The self-doping of PMAP was clearly shown by UV-vis-NIR and ESR. Meanwhile, the pyridinium salt was water-soluble and formed conductive films.

1-3. Experimental

General

NMR spectra were recorded on a JEOL JNM-ECS 400 spectrometer. Chemical shifts were reported in ppm on the δ scale relative to a residual solvent ($CDCl_3$: δ 7.26 for ^1H NMR and 77.0 ppm for ^{13}C NMR, CD_2Cl_2: δ 5.32 for ^1H NMR, D_2O: δ 4.79 for ^1H NMR) as an internal standard. 3-(Trimethylsilyl)-1-propanesulfonic acid sodium salt (-1.9 ppm) was used as an internal standard

for ^{13}C NMR in D_2O. An 85% aqueous phosphoric acid solution (0.00 ppm, sealed capillary) was used as an external standard for ^{31}P NMR. Infrared (IR) spectra were obtained with a JASCO FT/IR-6200 spectrometer. Mass spectra were measured on a JEOL JMS-DX-303 spectrometer using fast atom bombardment (FAB) mode. Inductively coupled plasma-mass spectrometry (ICP-MS) analysis was made on a SHIMADZU ICPS-8100. ESR spectrum was taken on a JEOL X-band spectrometer (JES-RE1XE). UV-vis-NIR spectra were recorded using a JASCO V-670 spectrophotometer. All reagents were purchased from commercial sources. $HPO(OEt)_2$ was used after distillation, and the other reagents were used without further purification. Milli-Q water was basically used except the synthesis of the monomer.

Synthesis

Diethyl (4-methoxy-3-nitrophenyl)phosphonate (3)

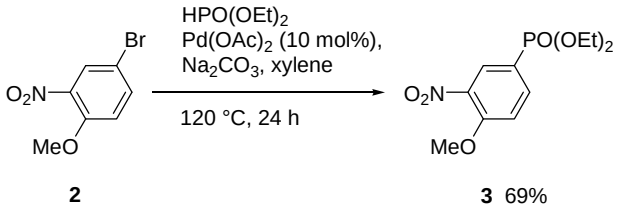

2 **3** 69%

To a dried two-necked round-bottomed flask were added 4-bromo-1-methoxy-2-nitrobenzene (**2**) (804 mg, 3.47 mmol), Na_2CO_3 (405 mg, 3.82 mmol), $Pd(OAc)_2$ (78 mg, 0.35 mmol), $HPO(OEt)_2$ (0.9 mL, 6.99 mmol), and xylene (3 mL) under nitrogen. The mixture was stirred at 120 °C for 24 h. After cooling to room temperature, the mixture was filtered through a short pad of Celite, which was washed with CH_2Cl_2. The filtrate was concentrated in vacuo, and the crude mixture was purified by silica gel column chromatography (1:1 hexane/ethyl acetate v/v) to give **3** together with $HPO(OEt)_2$. To remove $HPO(OEt)_2$, the mixture was further purified by Kugel-Rohr distillation to afford diethyl (4-methoxy-3-nitrophenyl)phosphonate (**3**) as a yellow oil (689 mg, 2.38 mmol, 69% yield).

3: ^1H NMR (400 MHz, $CDCl_3$) δ 1.30 (t, *J* = 6.9 Hz, 6H), 3.98 (s, 3H), 4.01-4.19 (m, 4H), 7.16 (dd, *J* = 8.5, 3.2 Hz, 1H), 7.92-7.98 (m, 1H), 8.19 (brd, *J* = 13.3 Hz, 1H); ^{13}C NMR (100 MHz, $CDCl_3$) δ 16.22 (d, *J* = 6.7 Hz), 56.70, 62.46 (d, *J* = 4.8 Hz), 113.49 (d, *J* = 15.3 Hz), 120.73 (d, *J* = 198.4 Hz), 129.13 (d, *J* = 12.5 Hz), 137.50 (d, *J* = 10.5 Hz), 139.45 (d, *J* = 18.2 Hz), 155.53 (d, *J* = 2.9 Hz); ^{31}P NMR (162 MHz, $CDCl_3$): δ 16.33; IR (ATR) ν 2984, 2907, 1610, 1531, 1247, 1012, 960 cm^{-1}; HRMS (FAB) *m*/*z* calcd for $C_{11}H_{17}NO_6P$ $[(M+H)^+]$ 290.0788, found 290.0789.

(3-Amino-4-methoxyphenyl)phosphonic acid hydrochloride (5)

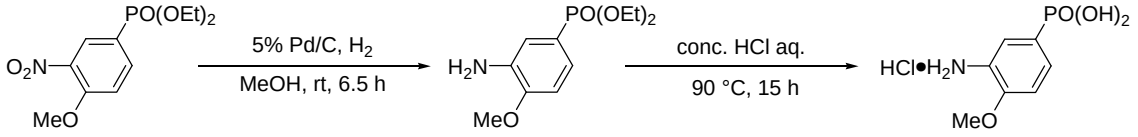

3 **4** **5** 2 steps 72%

To a dried two-necked round-bottomed flask were added phosphonate **3** (1.14 g, 3.9 mmol), MeOH (5 mL), and 5% Pd/C (88 mg) under nitrogen. Nitrogen was replaced with hydrogen by evacuation and purging for several times. After stirring under hydrogen at room temperature for 4.5 h, the mixture was filtered through a filter paper. The starting material **3** was still remained in the filtrate. To complete the reaction, this reaction was conducted again with 5% Pd/C (80 mg). After stirring for 2 h, the mixture was filtered through a short pad of Celite. The filtrate was concentrated in vacuo to give **4** as a brown liquid (0.83 g). The obtained product **4** was used without further purification.

4: ^{1}H-NMR (400 MHz, CD_2Cl_2) δ 1.26 (t, *J* = 6.9 Hz, 6H), 3.82 (brs, 2H), 3.86 (s, 3H), 3.94-4.06 (m, 4H), 6.83 (dd, *J* = 8.2, 4.1 Hz, 1H), 7.05 (dd, *J* = 1.8, 13.7 Hz, 1H), 7.11 (ddd, *J* = 1.8, 8.2, 13.3 Hz, 1H); ^{13}C-NMR (100 MHz, $CDCl_3$) δ 16.20 (d, *J* = 6.7 Hz), 55.41, 61.78 (d, *J* = 4.8 Hz), 109.76 (d, *J* = 18.2 Hz), 117.54 (d, *J* = 12.5 Hz), 119.34 (d, *J* = 192.7 Hz), 123.10 (d, *J* = 10.5 Hz), 135.94 (d, *J* = 19.2 Hz), 150.45 (d, *J* = 3.8 Hz); ^{31}P-NMR (162 MHz, CD_2Cl_2): δ 20.47; IR (ATR) ν 3467, 3329, 2980, 1620, 1584, 1511, 1285, 1223, 1015, 955 cm^{-1}; HRMS (FAB) *m*/*z* calcd for $C_{11}H_{19}NO_4P$ [(*M*+H)$^+$] 260.1046, found 260.1045.

To the thus-obtained product **4** (0.83 g) was added concentrated HCl (5 mL) at room temperature. The mixture was stirred at 90 °C for 15 h. Then, the solvent was removed. The resulting residue was dried in vacuo to give the product **5** (672 mg, 2.80 mmol, 2 steps 72% yield).

5: ^{1}H NMR (400 MHz, D_2O) δ 3.98 (s, 3H), 7.27 (dd, *J* = 8.7, 2.8 Hz, 1H), 7.70 (dd, *J* = 12.8, 1.8 Hz, 1H), 7.81 (ddd, *J* = 12.8, 8.7, 1.8 Hz, 1H); ^{13}C NMR (100 MHz, D_2O) δ 57.20, 113.41 (d, *J* = 16.3 Hz), 119.62 (d, *J* = 19.2 Hz), 124.60 (d, *J* = 190.3 Hz), 126.87 (d, *J* = 12.5 Hz), 134.22 (d, *J* = 10.5 Hz), 156.06 (d, *J* = 2.9 Hz); ^{31}P NMR (162 MHz, D_2O): δ 13.42; IR (KBr) ν 3359, 2847, 1622, 1502, 1114, 1004, 946 cm^{-1}; HRMS (FAB) *m*/*z* calcd for $C_7H_{11}NO_4P$ [(*M*+H)$^+$] 204.0420, found 204.0422.

PMAP

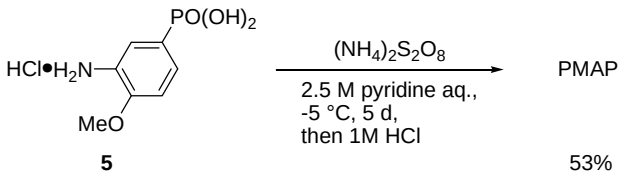

(3-Amino-4-methoxyphenyl)phosphonic acid hydrochloride (**5**) (1.0 g, 4.17 mmol) was dissolved in 2.5 M aqueous pyridine solution (5.32 mL, 13.3 mmol). After the solution was cooled to -5 °C, aqueous solution of $(NH_4)_2S_2O_8$ (1.19 g, 5.21 mmol in 4.6 mL of water) was added over 1 h at the same temperature. The reaction mixture was stirred at -5 °C for 5 d. Then, 1 M aqueous HCl solution (15 mL) was added to the mixture. The mixture was stirred for 10 min, and filtered. The resulting residue was washed with 0.2 M aqueous HCl solution (100 mL), water (100 mL), and Et_2O (10 mL). The residue was dried at 50 °C under the reduced pressure to give the desired polymer as a black solid (452 mg, 53% yield). IR (ATR) ν 1540, 1505, 1496, 1456, 1437, 1392, 1070 cm^{-1}; Anal. Calcd. for $C_{28}H_{31}N_4O_{16}P_4$ based on tetramer in the emeraldine structure: C, 41.86; H, 3.89; N, 6.97; Found: C, 43.70; H, 4.28; N, 6.95; composition of P atom was analyzed by ICP-MS, Anal. Calcd. for $C_{28}H_{31}N_4O_{16}P_4$ based on tetramer in the emeraldine structure: P, 15.48; Found: 12.03.

GPC analysis

Tandemly arranged two TSKgel α-M (7.8 mm I.D. x 30 cm, TOSOH) columns were used at column temperature 40 °C. A solution of ultrapure water/MeOH (8/2 = v/v) containing 20 mmol/L of Na_2CO_3 and 30 mmol/L of $NaHCO_3$ was used as an eluent at flow rate of 0.6 mL/min. Sample was diluted to 0.1 wt% with the eluent and filtered through a 0.5 μm cellulose acetate cartridge filter before injection (50 μL). A peak was detected by a UV detector (254 nm). Poly(styrene sulfonic acid)sodium salts (Mw 1260, 4210, 13500, 29500, 78400, 158000, 2350000) were used to make a calibration curve.

ESR measurement

ESR spectrum of an aqueous PMAP/pyridine solution (4.9×10^{-2} M based on the aniline unit) was measured at 298 K under non-saturating microwave-power conditions (0.998 mW) operating at 9.0464 GHz.

Electrical conductivity measurements

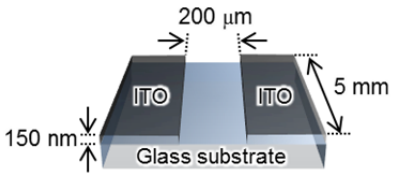

Figure 5. Schematic illustration of the electrode for electrical conductivity measurement.

The ITO/glass (shown in Figure 5) and glass substrates (26 x 26 mm) were ultrasonically washed with solvents in order of neutral detergent, water, acetone, ethanol, and desalted water twice for each process. They were stored in desalted water. Before usage they were dried by an air duster. The glass substrates were cleaned by UV-O_3 treatment (12W low pressure mercury lamp, flowing air) for 1 min after drying. The films were formed by drop-cast or spin-coating methods. The measurements of the electrical resistance for a two-probe method were conducted using a circuit tester (CUSTOM, CX-180N) under environmental conditions. For a four-probe method, the resistance measuring instrument (MITSUBISHI CHEMICAL ANALYTECH, Loresta-GP MCP-T610, Probe type: PSP linear) was employed to measure the sheet resistance. The sheet resistance was corrected with appropriate resistivity correction factors calculated by the software incorporated in the instrument.

Film formations

Drop-cast method for two-probe method : The aqueous 1 % (w/w) suspension or solution of the pyridinium salt of PMAP (ca. 4 μL) was dropped onto the ITO/glass substrate, which was dried with hot air from a dryer.

Drop-cast method for four-probe method : The aqueous 2% (w/w) solution of the pyridinium salt of PMAP (ca. 150 μL) was dropped onto the glass substrate, which was baked at 100 °C for 5 min under air.

Spin-coating method for film thickness measurement and SEM : The aqueous 2% (w/w) solution of the pyridinium salt of PMAP was spin-coated (3000 rpm, 20 sec) on the glass substrate, which was baked at 100 °C for 2 min under air.

Film thickness measurement

The film thickness was measured by a surface profiler (Kosaka Laboratory, surfcorder ET200). The measuring pressure and scanning speed were 10 μN and 20 μm/s, respectively. A gap was formed in the film by scratching it with the back of a box-cutter knife to expose the surface of the glass substrate (Figure 6a). The surface profile of the film was measured perpendicularly to the gap

to estimate the film thickness by averaging the obtained values (Figure 6b).

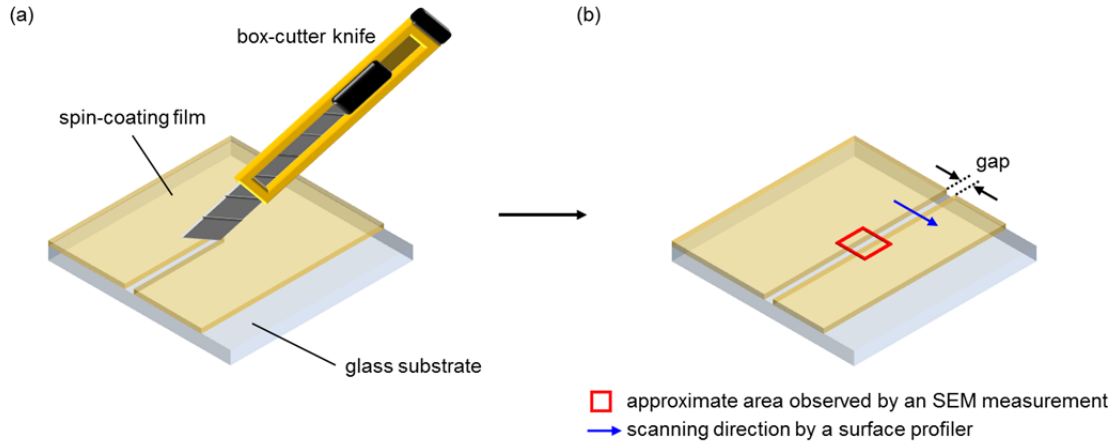

Figure 6. Schematic illustrations of (a) scratching the spin-coating film on a glass substrate with the back of a box-cutter knife and (b) the resulting gap with the film.

SEM analysis

The surface of the film that was used in the film thickness measurement (Figure 7a) was observed by a field emission scanning electron microscope (JEOL, JSM-6330FT) under reduced pressure (9.63×10^{-5} Pa). The accelerating voltage was 15.0 kV. The sample was coated with osmium using an osmium plasma coater (Filgen, OSMIUM PLASMA COATER OPC60A). The pressure, discharge current, and coating times were 0.8 Pa, 2.8 mA, and twice, respectively. Because a rough area was observed along sides of the gap, such area was employed to focus on the surface of the film (Figure 7a). Figures 7b and c show a boundary between a uniform and rough area (x 300 and x 5000, respectively). In a rough area, a lot of rod-like materials were observed. A typical enlarged view of them is shown in Figure 7d.

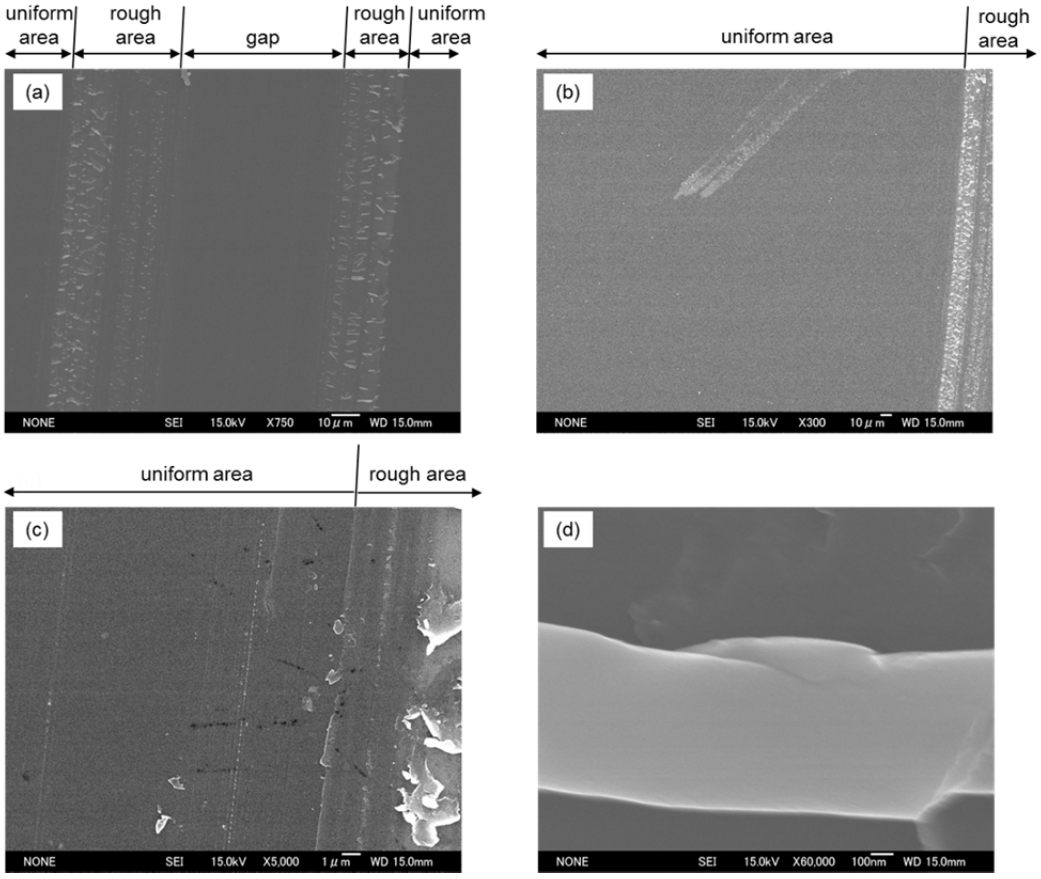

Figure 7. (a) Scanning electron micrograph of the surface of the film near the gap. The views of the boundary between a uniform and rough area {(b): x 300, (c): x 5000}. (d) A typical enlarged view of the rod-like materials observed in a rough area.

ICP-MS analysis

PMAP (10.1 mg) was dissolved in 3 mL of pH 9.0 borate buffer solution, which was diluted with H_2O in measuring flask to 100 mL in total. Quantification was carried out using calibration curve, which was prepared using four points of the diluted phosphorus standard solution (0, 5, 10, 50 ppm of P).

1-4. References and notes

1. (a) A. O. Patil, Y. Ikenoue, F. Wudl, A. J. Heeger, *J. Am. Chem. Soc.* **1987**, *109*, 1858-1859. (b) A. O. Patil, Y. Ikenoue, N. Basescu, N. Colaneri, J. Chen, F. Wudl, A. J. Heeger, *Synth. Met.* **1987**, *20*, 151-159. (c) M. S. Freund, B. Deore, Self-Doped Conducting Polymers, John Wiley & Sons Ltd, New York, 2007.
2. H. S. O. Chan, S. C. Ng, P. K. H. Ho, *Macromolecules* **1994**, *27*, 2159-2164.

3. (a) S. C. Ng, H. S. O. Chan, H. H. Huang, P. K. H. Ho, *J. Chem. Soc., Chem. Commun.* **1995**, 1327-1328. (b) H. S. O. Chan, P. K. H. Ho, S. C. Ng, B. T. G. Tan, K. L. Tan, *J. Am. Chem. Soc.* **1995**, *117*, 8517-8523.
4. Preparation: (a) R. J. Cooper, P. J. Camp, R. J. Gordon, D. K. Henderson, D. C. R. Henry, H. McNab, S. S. De Silva, D. Tackley, P. A. Tasker, P. Wight, *Dalton Trans.* **2006**, 2785-2793. (b) A. Mucha, A. Kunert, J. Grembecka, M. Pawełczak, P. Kafarski, *Eur. J. Med. Chem.* **2006**, *41*, 768-772.
5. (a) T. Hirao, T. Matsunaga, Y. Ohshiro, T. Agawa, *Synthesis* **1981**, 56-57. (b) T. Hirao, T. Matsunaga, N. Yamada, Y. Ohshiro, T. Agawa, *Bull. Chem. Soc. Jpn.* **1982**, *55*, 909-913.
6. Y. Xia, J. M. Wiesinger, A. G. MacDiarmid, *Chem. Mater.* **1995**, *7*, 443-445.
7. L. Dennany, P. C. Innis, F. Masdarolomoor, G. G. Wallace, *J. Phys. Chem. B* **2010**, *114*, 2337-2341.

Chapter 2. Development of a practical PMAP synthesis[P2]

2-1. Introduction

Chapter 1 summarized the initial synthesis of PMAP (Scheme 1a), which relied on multiple palladium-catalyzed reactions. However, this technique prevents widespread application of the material due to the prohibitive costs and difficulties that would be associated with increasing scale; both starting compound **2** (105.00 USD for 5 g from Aldrich) and the $Pd(OAc)_2$ catalyst (73.80 USD for 1 g from Aldrich) are particularly expensive reagents, while intermediate purification requires silica gel column chromatography and Kugel-Rohr distillation, cumbersome procedures for larger reactions.

To solve those issues, we chose the less expensive 4-bromoanisole **6** (166.00 USD for 500 g from Aldrich) as the new starting compound and $NiCl_2$ (39.50 USD for 50 g from Aldrich) as the phosphonate catalyst. Nitration of the resulting phosphonate compound **7** was envisioned to produce the key precursor **3**, which could then be used in the same manner as was developed in the original scheme. Although this new approach requires additional steps, it was thought to be much more practical overall. In addition to reviewing the modified scheme, this section describes the optimization of the hydrogenation and hydrolysis reactions that were retained from the previous synthesis.

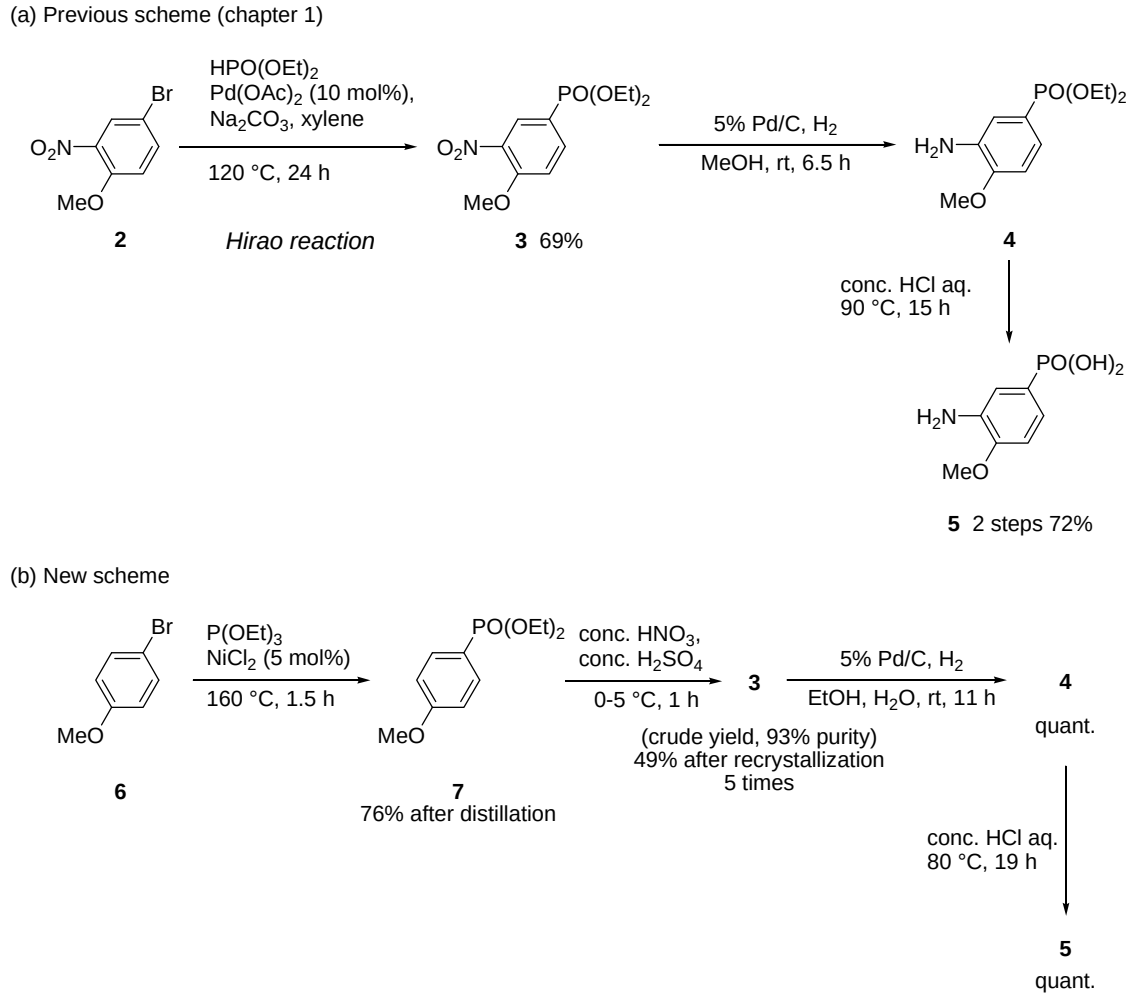

Scheme 1. Synthesis of the monomer **5** in (a) the scheme of chapter 1 and (b) the new scheme. (c) Polymerization of **5** to prepare PMAP.

2-2. Results and discussion

The initial $NiCl_2$-catalyzed step was carried out under solvent-free conditions at 160 °C.[1] At this temperature, the volatile ethyl bromide that is produced as a byproduct is removed immediately through the condenser tube. This reaction resulted in an 85:15 ratio of product **7** to starting material **6**, as shown by ^{1}H NMR of the crude mixture. Direct distillation was used to give product **7** in 76% yield.

The typical mixture of concentrated HNO_3 and H_2SO_4 was used to effect nitration in the next step, which proceeded well to give the nitrated compound **3**. However, ^1H NMR of the reaction mixture showed that the overreacted dinitrated product was also produced, present in a 7:93 ratio with respect to the target molecule. Purification was carried out by five repeat recrystallizations, which gave a final yield of 49%; silica gel column chromatography of the filtrate was also shown to be useful in isolating more of the target molecule.

Extending the reaction time of the hydrogenation of **3** initially described in chapter 1 allowed for quantitative acquisition of aniline **4**. Meanwhile, the production of monomer **5** could also be completed quantitatively by using concentrated HCl. Taking the previously listed yields into account, it was possible to isolate 10.3 g of **5** by starting with 25 g of **6**, all while avoiding column chromatography.

Polymerization of **5** was demonstrated on a gram scale; 4.0 g was polymerized with $(NH_4)_2S_2O_8$ in a 2.5 M aqueous pyridine solution at -5 °C for 5 d. Treatment with 1 M aqueous HCl gave PMAP in 49% yield (1.97 g) as a hard black solid. The obtained polymer had a *Mw* of 1.6 x 10^3 and a polydispersity index of 2.4, as determined by GPC. Elementary analysis was in good agreement with theoretical values. As before, the pyridinium salt was soluble in neutral water.

The absorption spectrum for an aqueous PMAP/pyridine complex in a solution of pH 4.93, formed in a 1:1 molar ratio with respect to the aniline unit, again showed the characteristic polaron band at about 420 nm and the free carrier tail from about 1000 nm (Figure 1, solid line). Analysis in a solution of pH 9.05 likewise gave a shoulder peak at around 430 nm and a broad localized polaron absorption band at around 700 nm, in addition to the free carrier tail (Figure 1, dashed line).[2] The electrical conductivity of the film formed from this solution was 0.27 S/cm, which is again in good agreement with chapter 1.

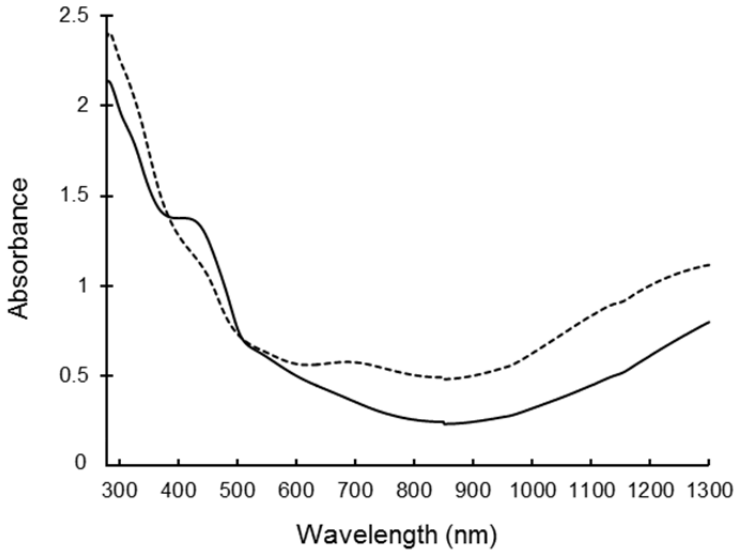

Figure 1. UV-vis-NIR spectra for PMAP/pyridine (1:1) in H_2O (pH 4.93) (solid line) and its pH 9.05 solution (dashed line) at 298 K (4.9×10^{-4} M based on the aniline unit).

In conclusion, a practical synthetic route for PMAP was successfully developed. In the new scheme, an inexpensive nickel C-P cross-coupling catalyst replaced the palladium one. This improved method for monomer synthesis was more appropriate for increasing scale than the previous one with respect to yield, purification, and cost. Polymerization was also performed on a gram scale. The pyridinium salt was again shown to be self-doping and water-soluble, and exhibited comparable conductivity.

2-3. Experimental

General

All reagents were purchased from commercial sources and were used without further purification. GPC analysis and electrical conductivity measurement were performed by using the same method in chapter 1. UV-vis-NIR spectra were recorded using a JASCO V-670 spectrophotometer. The measurements of the electrical resistance for a two-probe method were conducted using a circuit tester (CUSTOM, CX-180N) under environmental conditions.

Synthesis

Diethyl (4-methoxyphenyl)phosphonate (7)

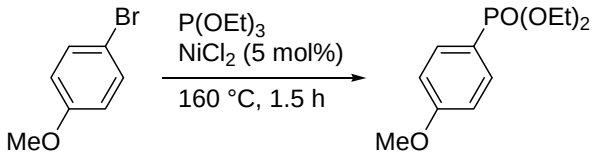

6 **7**
76% after distillation

4-Bromoanisole **6** (25.0 g, 0.134 mol) and dried $NiCl_2$ (0.87 g, 6.7 mmol) were added to a 200 mL dried round-bottomed flask attached to a Claisen adaptor with a Liebig condenser tube at room temperature. The mixture was then heated to 160 °C. To the mixture was slowly added $P(OEt)_3$ (32.5 mL, 0.188 mol) over 1 h. The formed ethyl bromide was removed immediately through the condenser tube. The reaction mixture was stirred at 160 °C for 30 min. After the reaction, the mixture was purified by distillation to give the phosphonate **7** as a colorless liquid (24.90 g, 0.102 mol, 76% yield). Chemical shifts of the ^{1}H NMR spectrum were identical with the reported values in chapter 1.

Diethyl (4-methoxy-3-nitrophenyl)phosphonate (3)

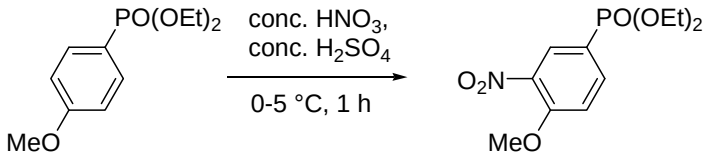

7 **3**
(crude yield, 93% purity)
49% after recrystallization
5 times

Concentrated H_2SO_4 (67 mL) was slowly added to the phosphonate **7** (22.39 g, 0.0917 mol) to be dissolved. After the reaction mixture was cooled to 0 °C, a mixed solution of concentrated HNO_3 (9.62 g, 0.0917 mol) and concentrated H_2SO_4 (9.47 g, 0.0917 mol) was added while maintaining the temperature 0 to 5 °C inside the flask over 30 min. The reaction mixture was stirred at the same temperature for 30 min. The reaction was quenched with ice water (300 g). The mixture was extracted with CH_2Cl_2 three times. The organic layer was washed with brine twice, an aqueous $NaHCO_3$ solution twice, and brine twice, dried with Na_2SO_4, and evaporated in vacuo to give the crude product [27.19 g, 103% crude yield (93% purity, determined by ^{1}H NMR)]. The crude product was recrystallized from Et_2O. After repeating the recrystallization five times, the combined nitrated compound **3** was obtained as yellow plate-like crystals (13.05 g, 0.045 mol, 49% yield). Chemical shifts of the ^{1}H NMR spectrum were identical with the reported values in chapter 1.

Diethyl (3-amino-4-methoxyphenyl)phosphonate (4)

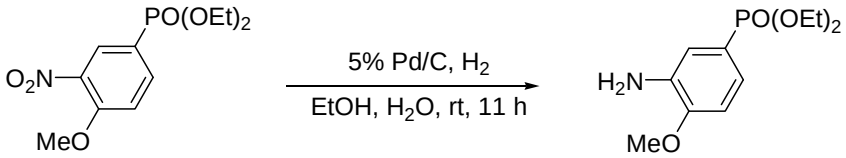

3 **4**
quant.

To a dried two-neck round-bottomed flask were added 5% Pd/C (470 mg), H_2O (1 mL), EtOH (30 mL), and phosphonate **3** (12.47 g, 0.043 mol) under nitrogen. Nitrogen was replaced with hydrogen by evacuation and purging several times. The mixture was stirred under hydrogen at room temperature for 11 h. During the reaction, purging of hydrogen was carried out every 2 h. The mixture was filtered through a short pad of Celite. The filtrate was concentrated in vacuo to give phosphonate **4** (11.18 g, 0.043 mol, quantitative). The obtained product **4** was used without further purification. Chemical shifts of the ^{1}H NMR spectrum were identical with the reported values in chapter 1.

(3-Amino-4-methoxyphenyl)phosphonic acid hydrochloride (5)

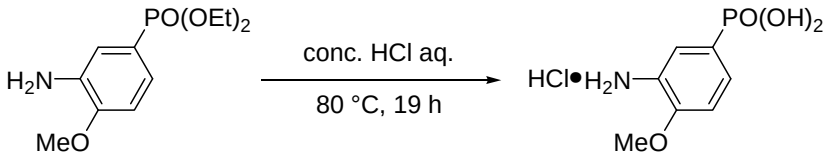

4 **5**
quant.

To the phosphonate **4** (11.18 g, 0.043 mol) was added concentrated HCl (31.4 g, 0.30 mol) at room temperature. The mixture was stirred at 80 °C for 19 h. Then, the solvent was removed. The resulting residue was dried in vacuo to give the product **5** (10.31 g, 0.043 mol, quantitative). Chemical shifts of the ^{1}H NMR spectrum were identical with the reported values in chapter 1.

PMAP

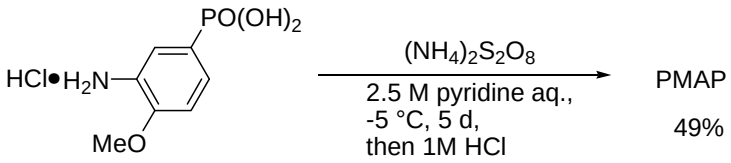

5

Monomer **5** (4.0 g, 16.69 mmol) was dissolved in 2.5 M aqueous pyridine solution (21.3 mL, 53.25 mmol). After the solution was cooled to -5 °C, an aqueous solution of $(NH_4)_2S_2O_8$ (4.76 g, 20.84 mmol in 18.4 mL of H_2O) was added in the range of -2 to -5 °C over 2.5 h. The reaction mixture was stirred at -5 °C for 5 d. Then, 1 M aqueous HCl solution (60 mL) was added to the mixture. The mixture was stirred for 10 min, and filtered. The resulting residue was washed with 0.2 M aqueous HCl solution (100 mL), H_2O (80 mL and 10 mL x 3), and Et_2O (30 mL). After drying in air, the residue was dried at 50 °C in vacuo to give the desired polymer as a black solid (1.97 g, 49% yield). Anal. Calc. for $C_{28}H_{31}N_4O_{16}P_4$ based on tetramer in the emeraldine structure: C, 41.86; H, 3.89; N, 6.97%. Found: C, 41.63; H, 4.30; N, 6.93%.

2-4. References and notes

1. Related conditions: (a) P. Tavs, *Chem. Ber.* **1970**, *103*, 2428-2436. (b) C. Yuan, H. Feng, *Synthesis* **1990**, 140-141.
2. (a) Y. Xia, J. M. Wiesinger, A. G. MacDiarmid, *Chem. Mater.* **1995**, *7*, 443-445.L. (b) Dennany, P. C. Innis, F. Masdarolomoor, G. G. Wallace, *J. Phys. Chem. B* **2010**, *114*, 2337-2341.

Chapter 3. PMAPE Synthesis[P3]

3-1. Introduction

The selective hydrolysis of diester **3**, an intermediate in the PMAP synthesis developed in chapters 1 and 2, with NaOH was conceived as a means to create the precursor for the synthesis of PMAPE (Figure 1). It was thought that analyzing the differences between the properties of PMAP and PMAPE that result from their being a di- and monoprotic acid, respectively, could provide insight into the structure-property relationship of the resulting polymers.

This chapter provides a description of the synthesis of the monomer 2-methoxyaniline-5-phosphonic acid monoethyl ester by this route, and then follows it by detailing the synthesis of PMAPE via oxidative polymerization and reviewing the properties of that material. This is the first example of a conducting self-doped polymer with a phosphonic acid monoester moiety.

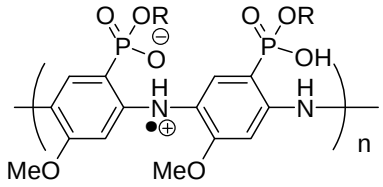

PMAP : R = H, PMAPE : R = Et

Figure 1. Structures of PMAP and PMAPE.

3-2. Results and discussion

Scheme 1 shows the developed synthetic route for PMAPE. Treatment of diester **3** with NaOH in MeOH-H_2O at 70 °C afforded the monoester **8** in 49% yield. Hydrogenation of this compound then gave the aniline monomer **9** (86% yield). This monomer was polymerized with $(NH_4)_2S_2O_8$ in a 2.5 M aqueous pyridine solution at -5 °C for 5 d, mirroring the PMAP polymerization conditions. Subsequent treatment with 1 M aqueous HCl solution gave PMAPE as a hard black solid (44% yield). The obtained polymer had a *Mw* of 4.3 x 10^3 and a polydispersity index of 2.2, as determined by GPC. As with PMAP, PMAPE only showed good solubility in basic aqueous solution, though the pyridinium salt was soluble in neutral water as well.

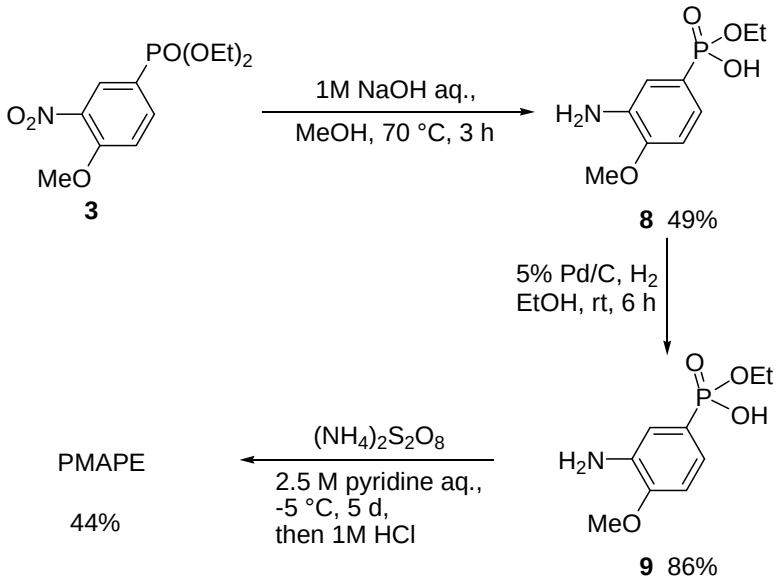

Scheme 1. Synthetic route of PMAPE.

Figure 2 shows the UV-vis-NIR spectrum of the obtained PMAP. The brown aqueous solution of the PMAPE/pyridine complex (in a 1:0.5 molar ratio with respect to the aniline unit) formed at a pH of 5.05 was analyzed initially. The complex gave a maximum absorption at 304 nm, while the latter peak at about 445 nm can be assigned as a polaron band. This material also shows a free carrier tail starting from around 1000 nm, again a sign that the target polymer was actually produced.[1]

As in the case with PMAP, an otherwise identical solution set to a more basic pH of 9.04 showed three maximum absorptions, this time at 316, 465, and 608 nm. In particular, the broad absorption around 608 nm is believed to result from a charge-transfer (CT) band.[1]

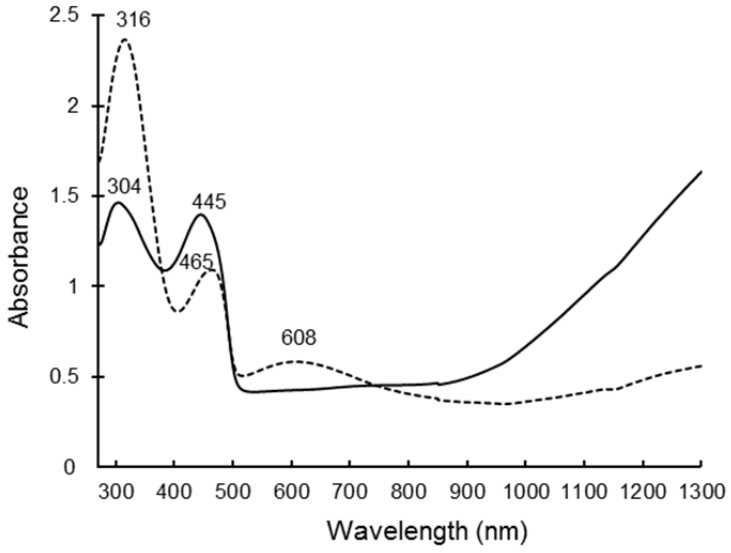

Figure 2. UV-vis-NIR spectra for PMAPE 1b at 298 K (4.3 x 10^{-4} M based on the aniline unit): PMAPE/pyridine (1:0.5) in H_2O (pH 5.05) (solid line) and in the pH 9.04 aqueous solution (dashed line).

The ESR spectrum of an aqueous solution of the PMAPE/pyridine complex, this time at a molar ratio of 1:1 with respect to the aniline unit, exhibited a single resonance line centered at around g = 2.0036 without hyperfine coupling (Figure 3). Again, this is characteristic of the delocalized free radicals of doped polyanilines.[2] When compared to PMAP, the PMAPE peak is broader and less intense.

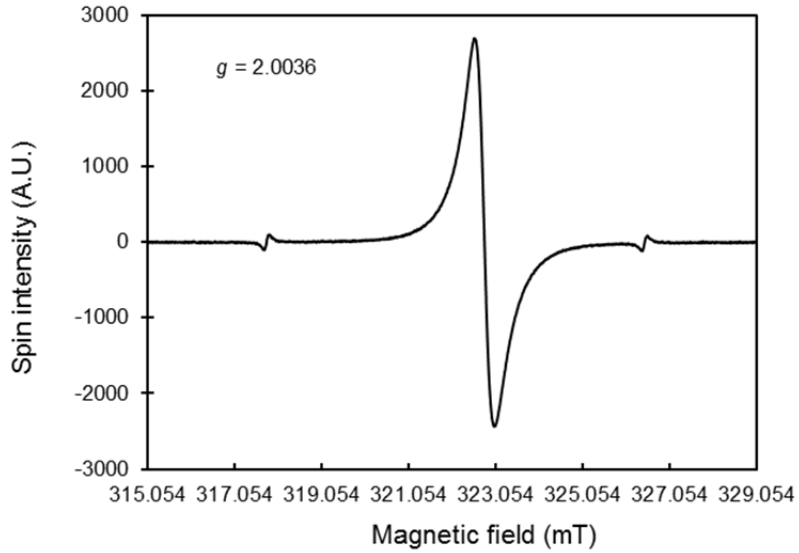

Figure 3. ESR spectrum for PMAPE/pyridine (1:1) in H_2O at 298 K (4.3 x 10^{-2} M based on the aniline unit).

The electrical resistance of the film was measured by a DC method (Table 1). The tested films were formed by drop-casting an aqueous 1% (w/w) solution of the pyridinium salt on a glass

substrate, onto which was placed a pair of ITO electrodes with a built-in gap (width: 200 μm, height: 150 nm; see Figure 5 of the chapter 1 Experimental). Two different compositions were tested by preparing aqueous solutions, which varied the molar ratio of pyridine to PMAPE. The electrical resistance of both films was 200 kΩ (Table 1), which corresponded to a conductivity of 1.3 S/m. Note that this is one order of magnitude smaller than the values obtained for PMAP (Table 1 in chapter 1).

Table 1 Electrical resistance and conductivity for the drop-cast films of the aqueous 1% (w/w) solution of the pyridinium salts of PMAPE.

Entry	Molar equivalents of pyridine[a]	Electrical resistance (kΩ)	Conductivity[b] (S/m)
1	1	200	1.3
2	2	200	1.3

[a] Based on the aniline unit.
[b] Conductivity was calculated on the assumption that the gap was filled with the polymer. Therefore, the obtained values are the minimum value.

Sheet resistance was measured by a four-point probe method. The tested film was formed by drop-casting an aqueous 2% (w/w) solution of the PMAPE/pyridine complex (at a molar ratio of 1:1 with respect to the aniline unit) on a glass substrate; an overall value of 4.1 x 10^6 Ω/□ was obtained.

The same solution used above was then spin-coated on a glass substrate to allow for surface analysis. An SEM image of the resulting surface is shown in Figure 4 in the Experimental, and demonstrated a uniformly formed surface.

In conclusion, the self-doped conducting polyaniline PMAPE was successfully synthesized via oxidative polymerization. UV-vis-NIR and ESR measurements clearly showed that self-doping was present in the sample, while the pyridinium salt was water-soluble and conductive when formed into a film.

3-3. Experimental

General

NMR spectra were recorded on a JEOL JNM-ECS 400 spectrometer. Chemical shifts were reported in ppm on the δ scale relative to a residual solvent ($CDCl_3$: δ 7.26 for ^1H NMR and 77.0 ppm for ^{13}C NMR, D_2O: δ 4.79 for ^1H NMR) as an internal standard. 3-(Trimethylsilyl)-1-propanesulfonic acid sodium salt (-1.9 ppm) was used as an internal standard for ^{13}C NMR in D_2O. An 85% aqueous phosphoric acid solution (0.00 ppm) was used as an external standard for ^{31}P NMR. IR spectra were obtained with a JASCO FT/IR-6200 spectrometer. Mass

spectra were measured on a JEOL JMS-DX-303 spectrometer using electron impact (EI) mode. ICP-MS analysis was made on a SHIMADZU ICPS-8100 by using the same method of chapter 1. ESR spectrum was taken on a JEOL X-band spectrometer (JES-RE1XE). UV-vis-NIR spectra were recorded on a JASCO V-670 spectrophotometer. All reagents were purchased from commercial sources. Milli-Q water was used except the synthesis of the monomer. GPC analysis, SEM analysis (Figure 5 for approximate observed area), electrical conductivity measurements and film formations by a drop-cast and a spin-coating were carried out by using the same method of chapter 1.

Synthesis

(4-Methoxy-3-nitrophenyl)phosphonic acid monoethyl ester (8)

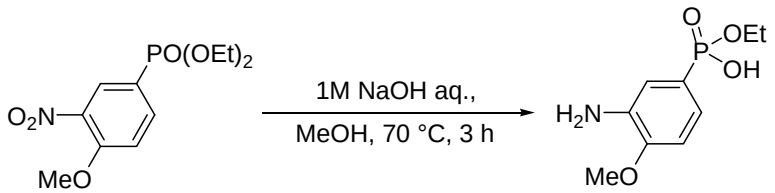

3 **8** 49%

To a round-bottomed flask were added diethyl(4-methoxy-3- nitrophenyl)phosphonate (**3**) (2.4 g, 8.3 mmol), MeOH (10 mL), and 1 M aqueous NaOH solution (9.1 mL) at room temperature. The mixture was stirred at 70 °C for 3 h. After concentration, 1 M aqueous HCl solution (ca. 10 mL to reach pH 1) was added to the mixture. The mixture was extracted with ethyl acetate. The organic layer was dried with Na_2SO_4 and evaporated in vacuo. The residue was purified by silica-gel column chromatography (1:10 MeOH/CH_2Cl_2, v/v) to give monoester **8** as a yellow solid (1.072 g, 4.1 mmol, 49% yield). Mp 103-104 °C (uncorrected); ^{1}H NMR (400 MHz, $CDCl_3$) δ 1.31 (t, *J* = 6.9 Hz, 3H), 4.00 (s, 3H), 4.06-4.13 (m, 2H), 7.11 (dd, *J* = 8.7, 3.2 Hz, 1H), 7.91 (ddd, *J* = 12.7, 8.7, 1.8 Hz, 1H), 8.19 (dd, *J* = 14.0, 1.8 Hz, 1H); ^{13}C NMR (100 MHz, CDCl3) δ 15.98 (d, *J* = 6.7 Hz), 56.62, 62.39 (d, *J* = 5.8 Hz), 113.46 (d, *J* = 15.3 Hz), 120.97 (d, *J* = 202.2 Hz), 128.67 (d, *J* = 13.4 Hz), 137.04 (d, *J* = 11.5 Hz), 139.07 (d, *J* = 19.2 Hz), 155.52 (d, *J* = 2.9 Hz); ^{31}P NMR (162 MHz, $CDCl_3$): δ 16.76; IR (ATR) ν 3069, 2988, 2949, 2908, 2847, 2255, 1699, 1613, 1530, 1352, 1283, 1163, 1023 cm^{-1}; HRMS (EI) *m*/*z* calcd for $C_9H_{12}NO_6P$ [(*M*+H)$^+$] 261.0402, found 261.0404.

2-Methoxyaniline-5-phosphonic acid monoethyl ester (9)

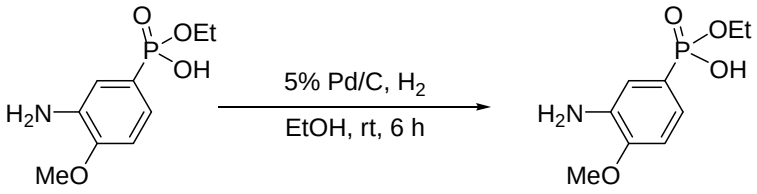

8 **9** 86%

To a three-necked round-bottomed flask were added monoester **8** (873 mg, 3.34 mmol), EtOH (20

mL), and 5% Pd/C (80 mg) under nitrogen. Nitrogen was replaced with hydrogen by evacuation and purging for several times. After stirring under hydrogen at room temperature for 6 h, water (50 mL) was added to the mixture. The mixture was filtered through a filter paper. The filtrate was concentrated in vacuo to give **9** as a gray solid (661 mg, 2.86 mmol, 86% yield). The obtained product **9** was used without further purification. Mp 202-203 °C (uncorrected); ^{1}H NMR (400 MHz, D_2O) δ 1.19 (t, *J* = 6.9 Hz, 3H), 3.80-3.89 (m, 2H), 3.99 (s, 3H), 7.26 (dd, *J* = 8.7, 3.2 Hz, 1H), 7.62 (dd, *J* = 12.6, 1.8 Hz, 1H), 7.72 (ddd, *J* = 12.5, 8.7, 1.8 Hz, 1H); ^{13}C NMR (100 MHz, D_2O) δ 16.18 (d, *J* = 5.8 Hz), 56.72, 61.70 (d, *J* = 4.8 Hz), 112.74 (d, *J* = 15.3 Hz), 120.72 (d, *J* = 19.2 Hz), 126.11 (d, *J* = 184.0 Hz), 126.14 (d, *J* = 11.5 Hz), 133.17 (d, *J* = 9.6 Hz), 154.72 (d, *J* = 2.9 Hz); ^{31}P NMR (162 MHz, D_2O): δ 14.6; IR (ATR) ν 2971, 2933, 2840, 2578, 2138, 1637, 1560, 1500, 1308, 1270, 1189, 1037 cm^{-1}; HRMS (EI) *m*/*z* calcd for $C_9H_{14}NO_4P$ [(*M*+H)$^+$] 231.0660, found 231.0660.

PMAPE

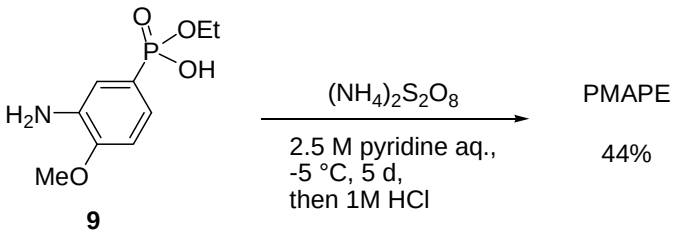

9

2-Methoxyaniline-5-phosphonic acid monoethyl ester (**9**) (540 mg, 2.33 mmol) was dissolved in 2.5 M aqueous pyridine solution (3.0 mL, 7.5 mmol). After the solution was cooled to -5 °C, aqueous solution of $(NH_4)_2S_2O_8$ (665 mg, 2.91 mmol in 2.6 mL of water) was added over 2.5 h at the same temperature. The reaction mixture was stirred at -5 °C for 5 d. Then, 1 M aqueous HCl solution (10 mL) was added to the mixture. The mixture was stirred for 10 min, and filtered. The resulting residue was successively washed with 0.2 M aqueous HCl solution (60 mL), water (60 mL), and Et_2O (10 mL). The residue was dried at 50 °C under the reduced pressure to give the desired polymer PMAP as a black solid (240 mg, 44%). IR (ATR) ν 2975, 1550, 1496, 1440, 1385, 1257, 1211, 1155, 1073, 1020, 917, 819 cm^{-1}; Anal. calcd. for $C_{36}H_{47}N_4O_{16}P_4$ based on tetramer in the emeraldine structure: C, 47.22; H, 5.17; N, 6.12; found: C, 44.20; H, 5.46; N, 5.57; composition of P atom was analyzed by ICP-MS, Anal. calcd. for $C_{36}H_{47}N_4O_{16}P_4$ based on tetramer in the emeraldine structure: P, 13.53; found: 12.71.

SEM analysis

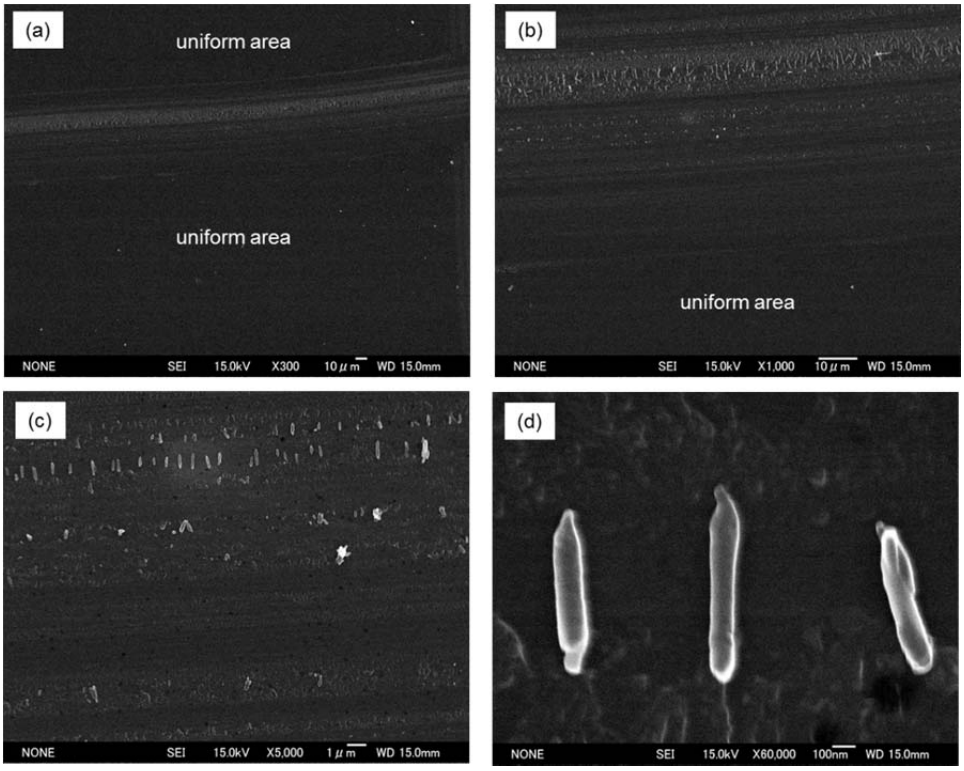

Figure 4. (a) Scanning electron micrograph of the surface of the film near the gap. The views of the boundary between a rough area resulted by scratching and a uniform area {(b): x 1000, (c): x 5000}. (d) A typical enlarged view of the rod-like materials observed in a rough area.

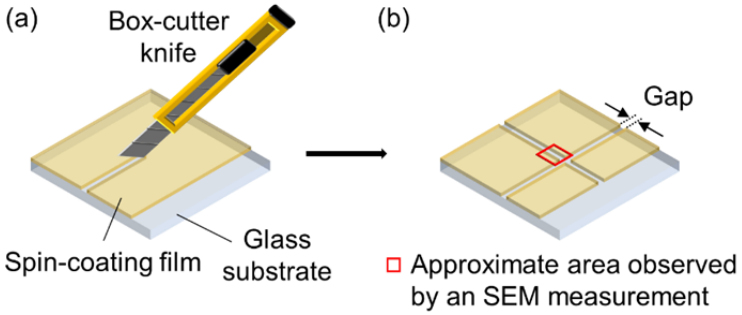

Figure 5. Schematic illustrations of (a) scratching the spin-coating film on a glass substrate with the back of a box-cutter knife and (b) the resulting gap in the film.

3-4. References and notes

1. Y. Xia, J. M. Wiesinger, A. G. MacDiarmid, *Chem. Mater.* **1995**, *7*, 443-445.
2. P. C. Innis, F. Masdarolomoor, G. G. Wallace, *J. Phys. Chem. B* **2010**, *114*, 2337-2341.

Chapter 4. Properties of PMAP and PMAPE: characterization and chemical oxidation and reduction[P4]

4-1. Introduction

In chapters 1-3, the author focused on integrating phosphonic acid moieties as dopants for polyaniline[1-3] and synthesized two self-doped polyanilines following this principle, PMAP and PMAPE (Figure 1). These are the first examples of self-doped polyaniline possessing a phosphonic acid unit attached directly to the polymer backbone. Self-doping was clearly demonstrated by UV-vis-NIR and ESR of the PMAP and PMAPE pyridinium salts, while conductivity measurements of their drop-casted films gave values of 0.19 and 0.01 S/cm, respectively. If these materials are to be applied outside of the laboratory, however, it is necessary to more fully characterize them, especially with respect to doping and electronic states. This chapter focuses on the thermostability, solid-state morphology, spin-coated film absorption and transparency, polaron delocalization, doping efficiency, and chemical oxidation and reduction of the polymers.

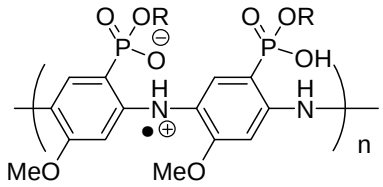

PMAP : R = H, PMAPE : R = Et

Figure 1. Structures of PMAP and PMAPE.

4-2. Results and discussion

4-2-1 *Thermal stability*

Thermogravimetric analysis (TGA) was conducted to investigate the thermal stability of PMAP and PMAPE. Figure 2 shows the results for both polymers under a nitrogen atmosphere. The mass change at low temperature (~100 °C) is attributed to volatilization of water contained in the polymers.[4,5] The polymers lost almost 10% of their mass by the time they reached 300 °C. Weight loss beyond this temperature did not accelerate significantly for PMAP; whatever loss did occur is presumably due to cleavage of the phosphonic acid moiety. On the other hand, a significant mass change was observed in this range for PMAPE, which might have been caused by decomposition of the ethylester moiety.

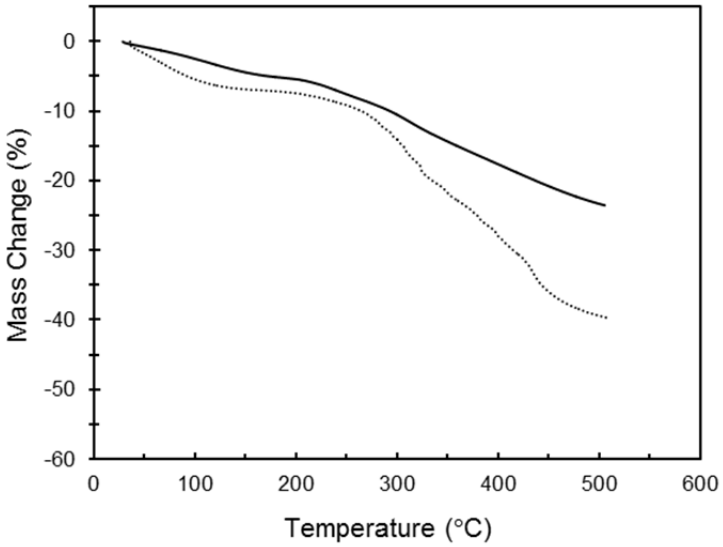

Figure 2. TGA curves for PMAP and PMAPE under a nitrogen atmosphere. Solid line: PMAP, dotted line: PMAPE.

4-2-2 *Morphology*

The morphological control of polyaniline has become especially important recently due to the various unique nanostructures (such as fibers, wires, rods, and tubes) that have been reported.[6-8] SEM was more fully employed by analyzing the powders of PMAP and PMAPE; the corresponding images are shown in Figures 3a-c and d-f, respectively. Samples were obtained by first drying the pastes that resulted from the polymerization, then crushing the resulting solids. Figures 3a and d show images at a magnification of 100, and reveal many sharp fragments for both samples. Figures 3b and e isolate individual fragments of PMAP and PMAPE at magnifications of 3000 and 800, respectively; these are further enhanced to a magnification of about 6000 in Figures 3c and f, respectively. The surfaces of the fragments are flat and smooth for both polymers. Note that the cross-sectional surfaces are a bit rougher, although nanostructured fibers were not observed.

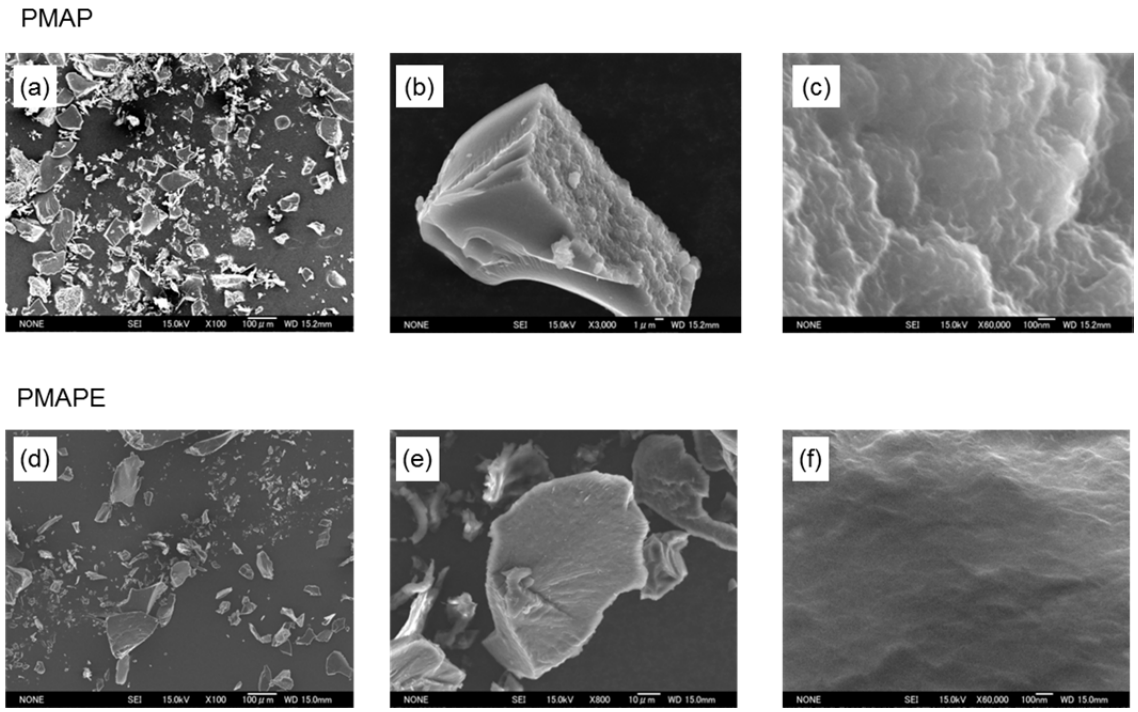

Figure 3. SEM images of PMAP {(a) 100x, (b) 3000x, (c) 60,000x and PMAPE (d) 100x, (e) 800x, (f) 60,000x. Scale bars in the images show as follows {(a) and (d): 100 μm, (b): 1 μm, (c) and (f): 100 nm, (e): 10 μm}.

4-2-3 *Electronic absorption and transparency*

The electronic absorption and transparency of the polymers were investigated using spin-coated films. These were formed on glass substrates using aqueous solutions of variable concentrations of the pyridinium salts, with molar ratios of 1:2 and 1:1 with respect to the aniline unit for PMAP and PMAPE, respectively. Once coated, the films were baked at 100 °C for 2 min under air.

The 2 wt% PMAP and PMAPE films gave thicknesses of 34 and 41 nm, respectively. UV-vis-NIR spectra of these films are shown in Figures 4a and b. Note that the shape of the spectra are similar to those observed for the aqueous solutions discussed in chapters 1 and 2. Characteristic polaron band peaks were observed at 444 and 472 nm for the PMAP and PMAPE complexes, respectively, values that are slightly red shifted when compared to the solution spectra.[9] As before, the spectra also exhibited free carrier tails over 1000 nm,[9] with maxima at 2073 and 2011 nm for PMAP and PMAPE, respectively.

Table 1 summarizes the transparency and thickness of the spin-coated films. Transparency maxima were measured at about 440 and 470 nm for the light brown PMAP and yellow-brown PMAPE films, respectively (Figure 5). However, note that the exact values, as well as the thickness, were highly dependent on the concentration of the base solution; PMAP and PMAPE 1% (w/w) solutions gave the highest transparency (90 and 86%, respectively) and the lowest thickness (13 and

12 nm, respectively).

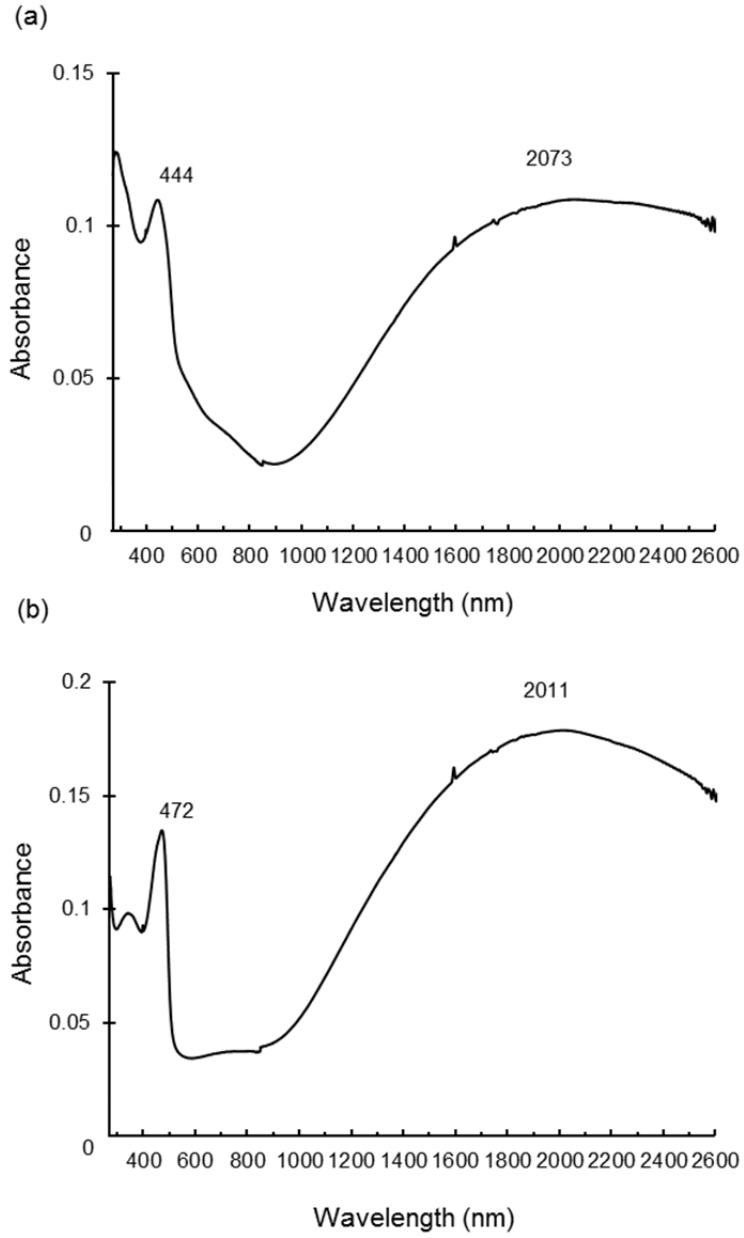

Figure 4. UV-vis-NIR spectra for the films formed by spin-coating with 2 wt% solutions of (a) PMAP/pyridine (1:2) and (b) PMAPE/pyridine (1:1).

Table 1. Thickness and transparency of the spin-coating film formed with the aqueous solution of the pyridinium salts of PMAP and PMAPE.

Polymer complexes	Concentration [% (w/w)]	Transparency (%) [Wavelength (nm)]	Thickness (nm)
PMAP/pyridine (1:2)	1	90 (438)	13
	2	78 (444)	34
	4	57 (441)	104
PMAPE/pyridine (1:1)	1	86 (470)	12
	2	73 (472)	41
	4	36 (469)	136

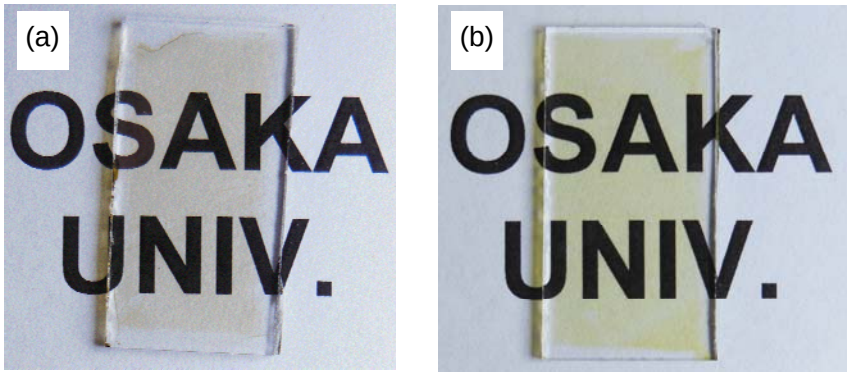

Figure 5. Photos of the spin-coating film formed with the aqueous 2% (w/w) solution of the pyridinium salt of (a) PMAP (molar ratio = 1:2 based on the aniline unit) and (b) PMAPE (molar ratio = 1:1 based on the aniline unit) on a glass substrate.

4-2-4 *ESR properties*

ESR was carried out to compare the delocalization of the charge carriers in PMAP and PMAPE. Figure 6 overlays the ESR spectra that had originally been presented in chapters 1 and 3. The PMAP sample has a peak-to-peak line width (ΔHpp) of 0.20 mT (2.0 G); meanwhile, g = 2.0036, with no hyperfine coupling. On the other hand, for the PMAPE sample, ΔHpp = 0.46 mT (4.6 G) and g = 2.0036, again without hyperfine coupling. The fact that ΔHpp is smaller for PMAP than PMAPE suggests that the PMAP polaron is more delocalized.[10-12] This is consistent with the conductivity results from chapters 1 and 3.

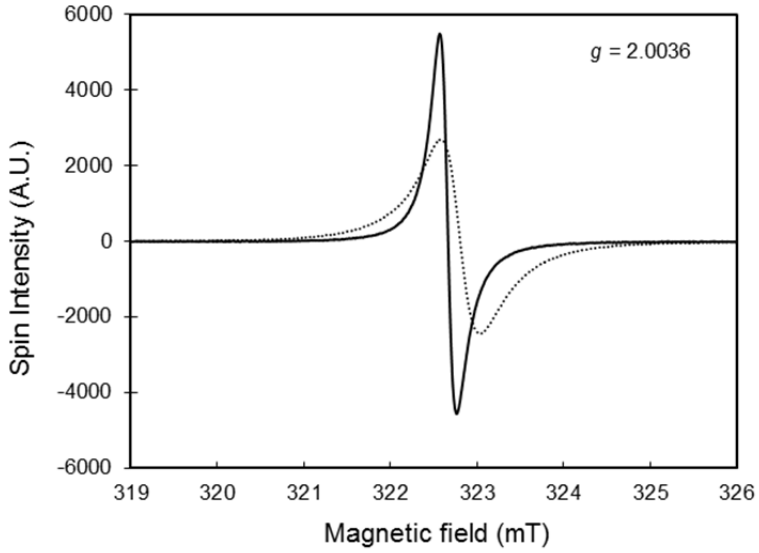

Figure 6. ESR spectra for PMAP/pyridine (1:2) (solid line, 4.9×10^{-2} M based on the aniline unit) and PMAPE/pyridine (1:1) (dotted line, 4.3×10^{-2} M based on the aniline unit). The spectra were adapted from chapters 1 and 3.

4-2-5 *Doping efficiency*

Polymer doping efficiency was investigated by X-ray photoelectron spectroscopy (XPS). Figures 7a and b show the spectra for PMAP and PMAPE, respectively. The N 1s core-level spectra were fitted to potential components; protonated ($–NH_2^+–$, $–N^+H=$), radical cation ($– N^{\bullet+}–$), neutral amine (–NH–), and imine (–N=) nitrogen sites were identified at 402.6, 400.6, 399.0, and 398.2 eV, respectively. These positions are comparable to previously reported values.[10-12]

The nitrogen area ratios are summarized in Table 2. The doping level corresponds to the area ratio for the radical cation nitrogen ($–N^{\bullet+}–$) sites, which were 48 and 26% for PMAP and PMAPE, respectively (Table 2). The greater value for PMAP likely results from the diprotic nature of the phosphonic acid moiety, and is consistent with the conductivity results from chapters 1 and 3.

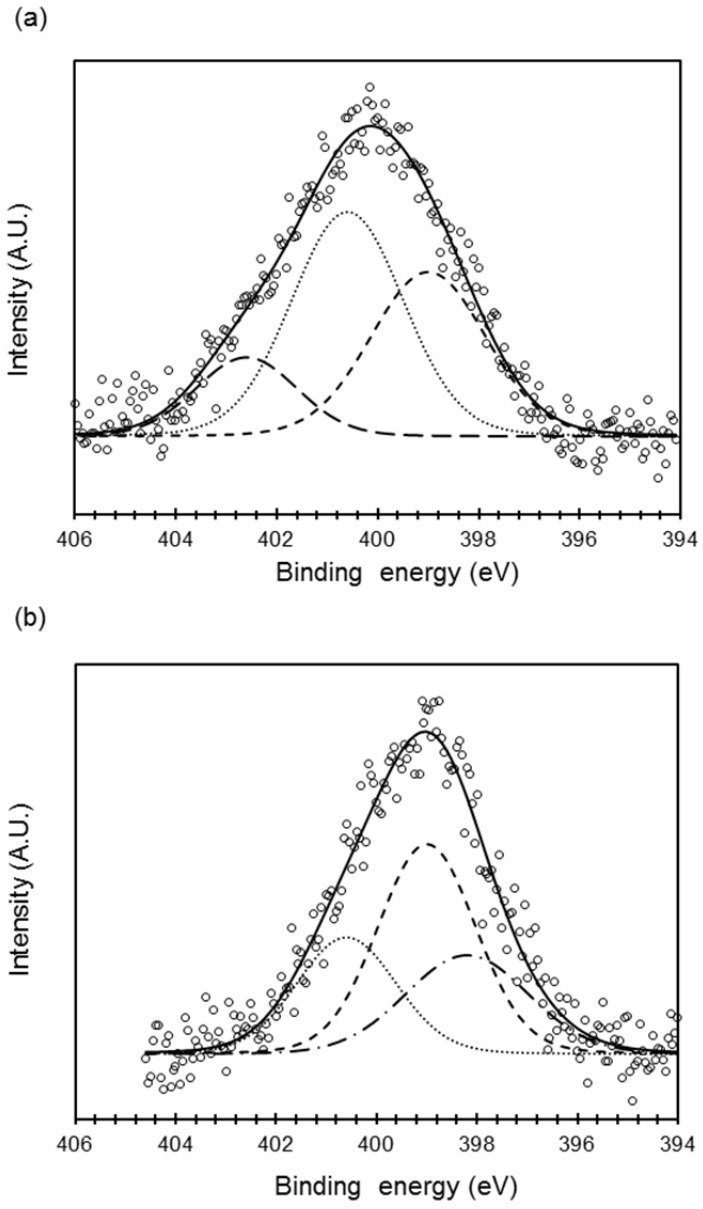

Figure 7. N 1s XPS spectra of (a) PMAP and (b) PMAPE. Measured data: white circles, its deconvoluted spectra (long-dashed line: protonated nitrogen, dotted line: radical cation nitrogen, dashed line: neutral amine, and long-dashed dotted line: neutral imine), and their convoluted spectra of the deconvoluted ones: solid line. Binding energies were referenced to the Ag $3d_{5/2}$ peak at 368.2 eV. The spectra are shown here after subtracting their backgrounds.

Table 2. Area ratio of the components resulting from the deconvolution of N 1s XPS spectra and doping level of PMAP and PMAPE.

Polyaniline	Area ratio (%)			
	402.6 eV $-NH^{2+}-$, $-N^{+}H=$	400.6 eV $-N^{\bullet+}-$	399.0 eV $-NH-$	398.2 eV $-N=$
PMAP	15	48	36	0
PMAPE	0	26	46	27

4-2-6 *Redox transformations*

Chemical oxidation and reduction of the produced PMAP and PMAPE were tested in order to better understand the redox behavior of the polymers. Reactions were followed by UV-vis-NIR spectroscopy. Cyclic voltammetry (CV) data was also obtained (Figures 10 and 11 in the Experimental).

Aqueous borate buffer solutions with a pH of 9.0 consisting of either PMAP or PMAPE (4.9 x 10^{-2} and 4.3 x 10^{-2} M with respect to the aniline unit, respectively) were treated with $(NH_4)_2S_2O_8$ (Figure 8). The color of the brown PMAP solution decreased somewhat in intensity, but did not otherwise exhibit any intense changes. Three equivalents of the oxidant did however decrease the intensities of the characteristic delocalized polaron band at 440 nm and localized emeraldine salt polaron band at 677 nm, as well as completely eliminate the free carrier tail above about 1000 nm (Figure 8a). Further addition of the oxidant did not induce any notable spectral change. PMAPE, on the other hand, underwent drastic color change, going from brown to purple, and finally to green as more oxidant was added. Three equivalents decreased the intensity of the delocalized emeraldine salt polaron band at 476 nm, while also completely eliminating the free carrier tail above about 1000 nm. Furthermore, the oxidized form was generated, as evidenced by the appearance of a characteristic peak at 540 nm (Figure 8b); similar results were reported for PMAS.[13] In this case, the more oxidant that was added, the more the peak intensities decreased.

The same borate buffer solutions used in the experiment above were also treated with $N_2H_4 \cdot H_2O$ (Figure 9). In both cases, the color intensity of the brown solutions decreased. The spectra of these reactions are shown in Figures 9a and b, respectively. The characteristic delocalized polaron band (PMAP: 440 nm, PMAPE: 476 nm), localized emeraldine salt polaron band (PMAP: 677 nm), benzenoid to quinoid CT band (PMAPE: 609 nm), and free carrier tails (above about 1000 nm for both samples) were all disappeared during the reduction. The resulting absorption spectra mainly consisted of $\pi-\pi^*$ transitions (PMAP: ~300 nm, PMAPE: ~330 nm), indicating the generation of the reduced forms; again, this is consistent with previous reports for PMAS.[14]

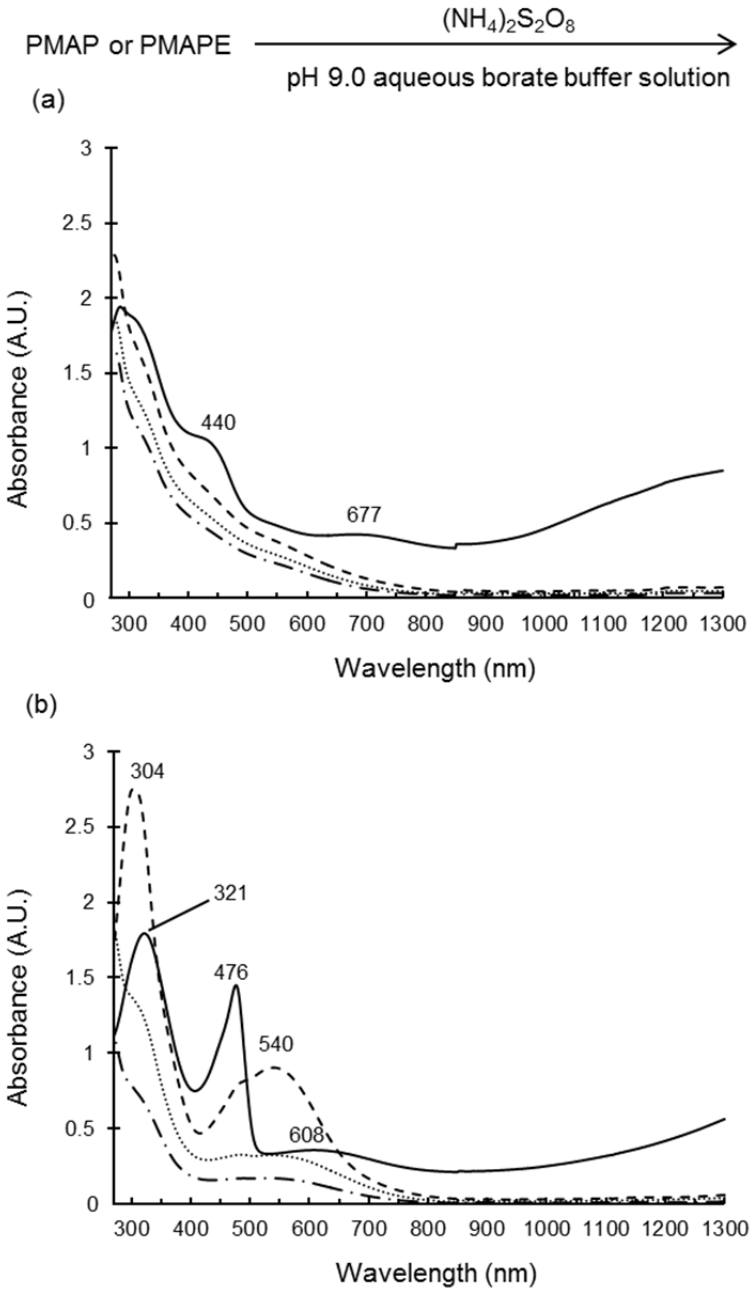

Figure 8. UV-vis-NIR spectral changes of (a) PMAP and (b) PMAPE with $(NH_4)_2S_2O_8$ in pH 9.0 aqueous borate buffer solution {before the reaction: solid line, 1st (3 eq.): dashed line, 2nd (7 eq., total 10 eq.): dotted line, 3rd (10 eq., total 20 eq.): longed dotted line}.

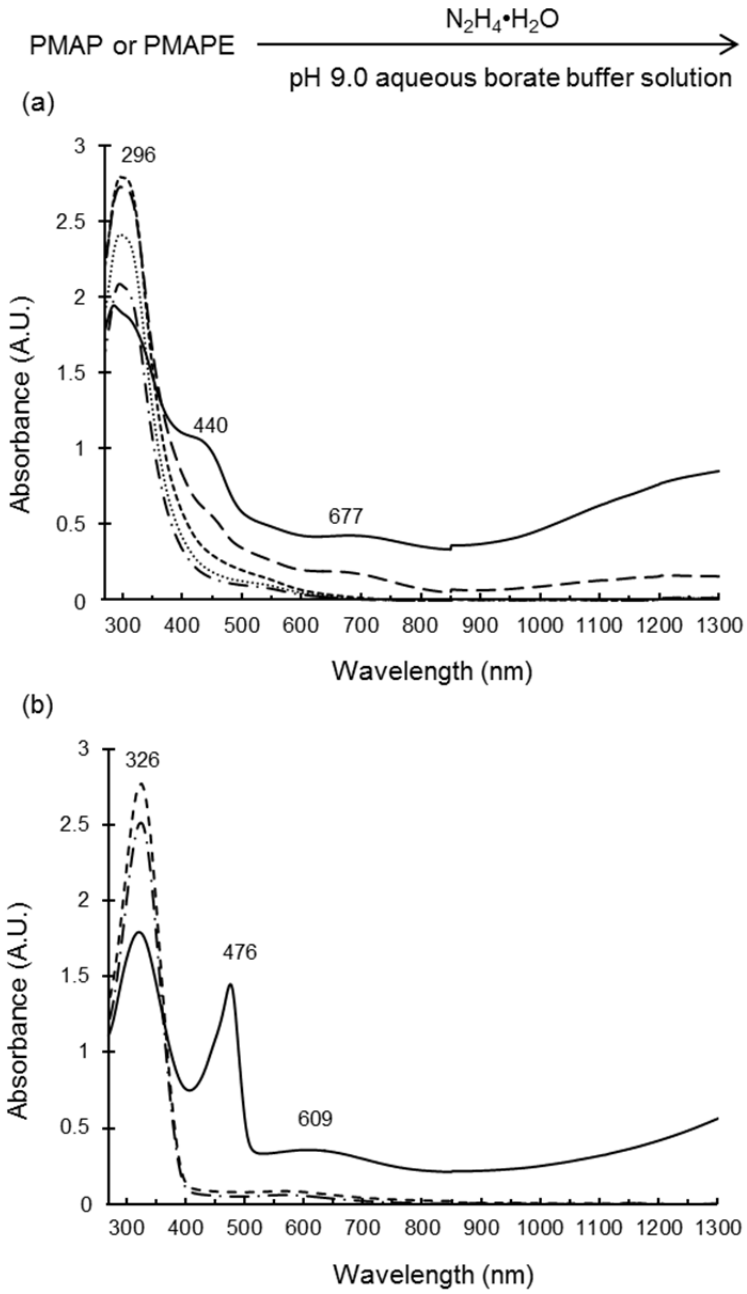

Figure 9. UV-vis-NIR spectral changes of (a) PMAP and (b) PMAPE with $N_2H_4 \cdot H_2O$ in pH 9.0 aqueous borate buffer solution. For PMAP, before the reaction: solid line, 1st (8 eq.): long-dashed line, 2nd (42 eq., total 50 eq.): short-dashed line, 3rd (50 eq., total 100 eq.): dotted line, and 4th (50 eq., total 150 eq.): long-dashed dotted line. For PMAPE, before the reaction: solid line, 1st (10 eq.): short-dashed line, and 2nd (40 eq., total 50 eq.): long-dashed dotted line.

In conclusion, the various properties of the synthesized PMAP and PMAPE polymers were assessed and compared to each other. Both were moderately thermally stable below 300 °C, up to which point almost 10% weight loss was observed. However, PMAPE lost significantly more mass above 300 °C. Furthermore, characteristic fiber, tube, or other nanostructures were not observed upon SEM analysis of the polymer powders. In addition, the UV-vis-NIR absorption spectra of the spin-coated films showed characteristic polaron bands and free carrier tails. Unsurprisingly, the transparency and thickness of the spin-coated films depended on the concentrations of the solutions used to manufacture them; the lowest concentration of 1% (w/w) gave high transparencies of 90 and 86% for PMAP and PMAPE, respectively. Meanwhile, ESR spectra suggested greater delocalization for the PMAP polaron than for the PMAPE one. Similarly, XPS experiments indicated a greater doping efficiency for PMAP, likely due to the diprotic nature of the phosphoric acid moiety. Finally, the oxidation and reduction capacities of the two polymers were assessed using $(NH_4)_2S_2O_8$ and $N_2H_4 \cdot H_2O$, respectively.

4-3. Experimental

General

All reagents were purchased from commercial sources and used without further purification. PMAP and PMAPE were prepared by procedures of chapters 1-3. Milli-Q water was used for the spectral measurements. pH 9.0 aqueous borate buffer solution was prepared by the following method: $B(OH)_3$ (3.09 g, 0.05 mol) was dissolved in Milli-Q water (90 mL). After that, 2 M aqueous NaOH solution was added to the solution to prepare pH 9.0 (0.5 M). UV-vis-NIR spectra were recorded on a JASCO V-670 spectrometer.

TGA

TGA was recorded on an SII TG/DTA6200 analyzer. Samples were put in open aluminum pan and measured under a nitrogen atmosphere (flow rate 150 mL/min).

SEM measurements

The powder of PMAP and PMAPE was put on a carbon tape. The SEM images were observed on a JEOL JSM-6335.

Film transparency measurements

Spin-coating film formation on glass substrates was carried out by the same method of chapter 1. The transparency of the spin-coating film of the pyridinium salt of PMAP and PMAPE was measured by UV-vis-NIR spectroscopy, where the substrate was cut as illustrated in Figure 4 before the measurement.

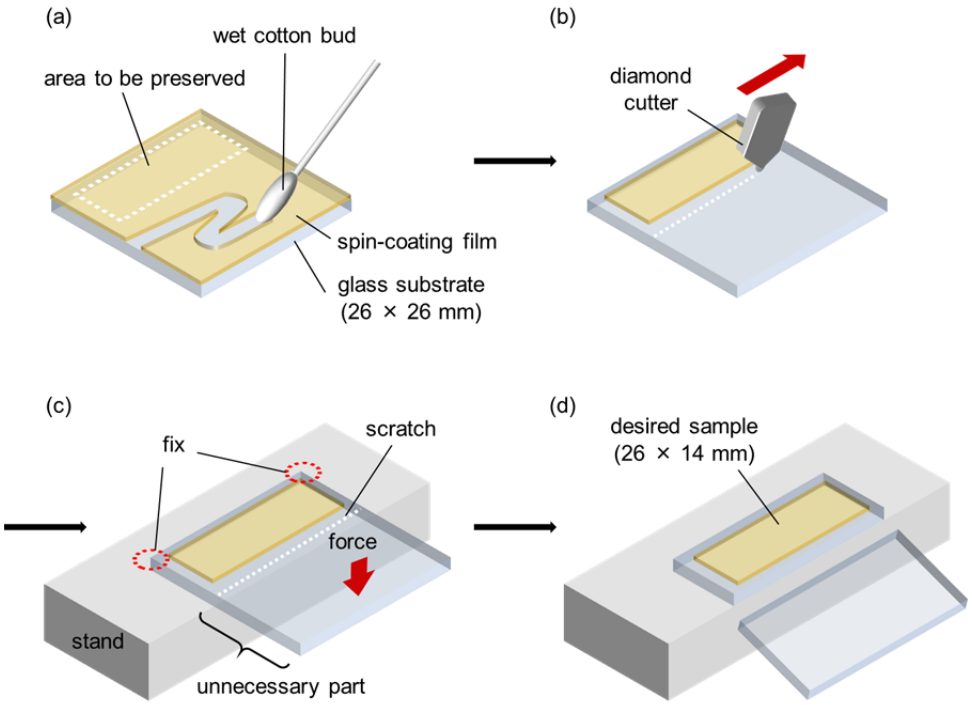

Figure 4. Schematic illustration showing how to cut a glass substrate (26 x 26 mm) with spin-coating film for the film transparency measurement. (a) Extra area of the spin-coating film was wiped off using a cotton bud wet with desalted water. (b) The glass substrate was scratched with a diamond cutter along the long side of the film. (c) The substrate was mounted on a stand, where the resulting scratch was located on the stand as shown above, and cut by applying a force perpendicular to the unnecessary part of the substrate (d) to give a desired sample (26 x 14 mm).

Film thickness measurements

The film thickness was measured by a surface profiler (Kosaka Laboratory, surfcorder ET200). The measuring pressure and scanning speed were 10 μN and 20 μm/s, respectively. Gaps were formed in the film by scratching it with the back of a box-cutter knife to expose the surface of the glass substrate (Figure 5a). The surface profile of the film was measured perpendicularly to the gap to estimate the film thickness by averaging the obtained values (Figure 5b).

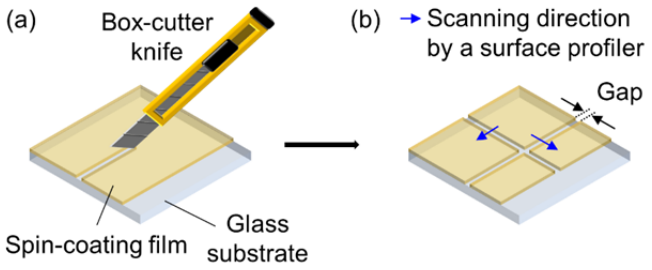

Figure 5. Schematic illustrations of (a) scratching the spin-coating film on a glass substrate with the back of a box-cutter knife and (b) the resulting gap in the film.

XPS measurements

The XPS measurements were carried out with an X-ray photo-emission spectrometer (SHIMADZU/Kratos, AXIS-165x) in an ultrahigh-vacuum chamber (2.3-9.3 × 10^{-9} Torr) at room temperature. The monochromatic Al Kα line of 1486.6 eV was employed as an X-ray source. The tube current, tube voltage, and pass energy were set at 12 mA, 15 kV, and 160 eV, respectively. Before recording the spectra, the sample surfaces were cleaned by argon-ion etching. The emission current and argon gas pressure were 15 mA and 1.2-1.7 x 10^{-7} Torr, respectively. The binding energies were calibrated using Ag $3d_{5/2}$ line (368.2 eV).[15] The intensity (counts/s) was corrected for quantitative analysis using appropriate transmission values supplied by the instrument manufacturer. Peak analysis of the obtained spectra was conducted using an analysis software (Light Stone, OriginPro 9.0J). Background subtraction was performed by subtracting linear function from the data to remove the gradient of the spectra. To deconvolute the N 1s spectra, they were fitted with Voigt functions, where Lorentzian width was fixed to 0.25 eV.

Redox transformations

i) *Oxidation reaction*

PMAP (10 mg, 0.049 mmol based on the aniline unit) was dissolved in 1 mL of pH 9.0 aqueous borate buffer solution under air at room temperature. $(NH_4)_2S_2O_8$ was added to the stirring solution in three parts {1st: 3 eq. (33 mg, 0.15 mmol), 2nd: 7 eq. (79 mg, 0.34 mmol), 3rd: 10 eq. (112 mg, 0.49 mmol)}. After every addition, 40 μL of solution was sampled by micropipette and then diluted with 4 mL of pH 9.0 aqueous borate buffer solution. The UV-vis-NIR spectra for the solutions were measured to monitor the reaction. The similar procedure was employed for PMAPE, where the amount of PMAPE (10 mg, 0.043 mmol based on the aniline unit) and the molar equivalents of $(NH_4)_2S_2O_8$ are same {1st: 3 eq. (29 mg, 0.13 mmol), 2nd: 7 eq. (67 mg, 0.29 mmol), 3rd: 10 eq. (96 mg, 0.42 mmol)}, but the solution was further diluted by half for the UV-vis-NIR measurements.

ii) *Reduction reaction*

The similar procedure to the oxidation reaction was employed for PMAP and PMAPE by use of $N_2H_4{\cdot}H_2O$ instead of $(NH_4)_2S_2O_8$. In the reduction reaction of PMAP, $N_2H_4{\cdot}H_2O$ was added in four parts {1st: 8 eq. (20 μL, 0.41 mmol), 2nd: 42 eq. (99 μL, 2.04 mmol), 3rd: 50 eq. (119 μL, 2.45 mmol), 4th: 50 eq. (119 μL, 2.45 mmol)}. In the reduction reaction of PMAPE, $N_2H_4{\cdot}H_2O$ was added in two parts 1st: 10 eq. (21 μL, 0.43 mmol), 2nd: 40 eq. (84μL, 1.73 mmol)}.

iii) *CV spectra*

CV spectra were measured by using a BAS-CV-50W voltammetric analyzer with glassy carbon electrode BAS GCE (6.0 x 1.6 mm). The solution for measurement was prepared by the following procedure. 1M aqueous NaCl solution was prepared with deionized water degassed by supersonic. PMAP: PMAP (5 mg) and 2.5 M aqueous pyridine solution (60 μL) were diluted by 1M aqueous NaCl solution (10 mL). PMAPE: PMAPE (5.7 mg) and 2.5 M pyridine (30 μL) were diluted by 1M aqueous NaCl solution (100 mL). CV spectra were measured under mild argon bubbling with scan rate 50 mV/sec (Figure 10). The neutral solutions were prepared by additions of 1M aqueous NaOH solution (Figure 11).

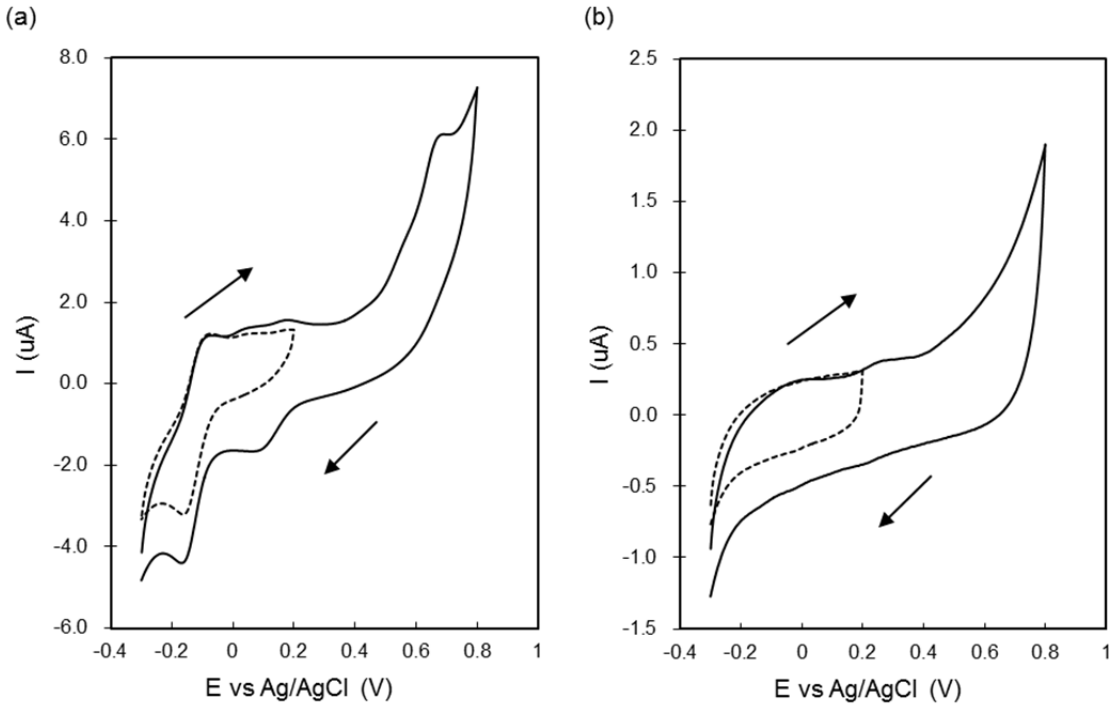

Figure 10. CV spectra of (a) PMAP/pyridine (1:6) in 1 M aqueous NaCl solution (2.5 x 10^{-3} M based on the aniline unit, pH 6.05) and (b) PMAPE/pyridine (1:3) in 1 M aqueous NaCl solution (2.5 x 10^{-4} M based on the aniline unit, pH 6.13), solid line: between -0.3 V and 0.8 V, dashed line: between -0.3 V and 0.2 V. Arrows show the direction of potential scan.

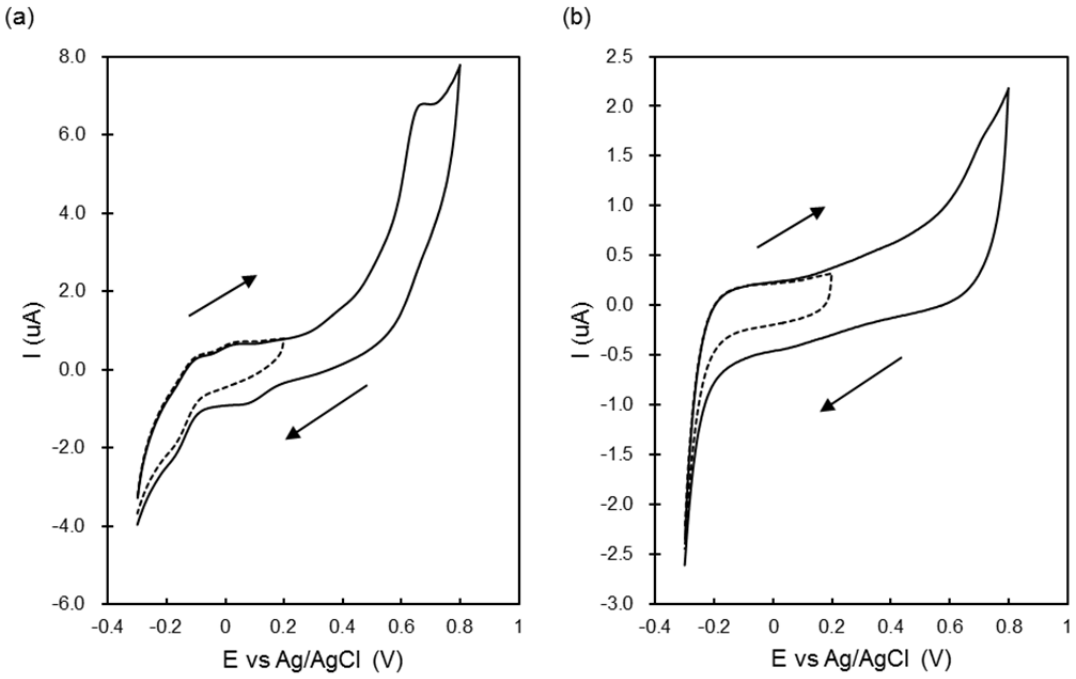

Figure 11. CV spectra of (a) PMAP/pyridine (1:6) in 1 M aqueous NaCl solution (2.5 x 10^{-3} M based on the aniline unit, pH 7.05) and (b) PMAPE/pyridine (1:3) in 1 M aqueous NaCl solution (2.5 x 10^{-4} M based on the aniline unit, pH 7.24), solid line: between -0.3 V and 0.8 V, dashed line: between -0.3 V and 0.2 V. Arrows show the direction of potential scan.

4-4. References and notes

1. S. C. Ng, H. S. O. Chan, H. H. Huang, P. K. H. Ho, *J. Chem. Soc. Chem. Commun.* **1995**, 1327-1328.
2. H. S. O. Chan, P. K. H. Ho, S. C. Ng, B. T. G. Tan, K. L. Tan, *J. Am. Chem. Soc.* **1995**, *117*, 8517-8523.
3. H. S. O. Chan, S. C. Ng, P. K. H. Ho, *Macromolecules* **1994**, *27*, 2159-2164.
4. E. C. Gomes, M. A. S. Oliveira, *Am. J. Polym. Sci.* **2012**, *2*, 5-13.
5. F. Masdarolomoor, P. C. Innis, S. Ashraf, G. G. Wallace, *Synth. Met.* **2005**, *153*, 181-184.
6. G. Ćirić-Marjanović, *Synth. Met.* **2013**, *177*, 1-47.
7. S. Bhadra, D. Khastgir, N. K. Singha, J. H. Lee, *Prog. Polym. Sci.* **2009**, *34*, 783-810.
8. J. Huang, R. B. Kaner, *Chem. Commun.* **2006**, 367-376.
9. Y. Xia, J. M. Wiesinger, A. G. MacDiarmid, *Chem. Mater.* **1995**, *7*, 443-445.
10. S.-A. Chen, G.-W. Hwang, *J. Am. Chem. Soc.* **1995**, *117*, 10055-10062.
11. I. Yamaguchi, S. Shigesue, M. Sato, *React. Funct. Polym.* **2009**, *69*, 91-96.
12. S.-A. Chen, G.-W. Hwang, *Macromolecules* **1996**, *29*, 3950-3955.

13. L. A. P. Kane-Maguire, J. A. Causley, N. A. P. Kane-Maguire, G. G. Wallace, *Curr. Appl. Phys.* **2004**, *4*, 394-397.
14. Y. Pornputtkul, E. V. Strounina, L. A. P. Kane-Maguire, G. G. Wallace, *Macromolecules* **2010**, *43*, 9982-9989.
15. J. F. Moulder, W. F. Stickle, P. E. Sobol, K. D. Bomben, Handbook of X-ray Photo-electron Spectroscopy, Perkin-Elmer Corporation, Eden Prairie, Minnesota, 1992.

Chapter 5. pH dependence of polaron delocalization in aqueous solutions of PMAP and PMAPE[P5]

5-1. Introduction

The main chain conformation of acid-doped emeraldine salts of polyaniline significantly impacts conductivity.[1] Those taking an extended coil conformation show much higher conductivity compared to those in the compact coil conformation (Figure 1a).[1] Therefore, investigation of the conformation is important.

Furthermore, polyanilines that are not doped with a sufficiently strong acid do not exhibit conductivity, further complicating their function under basic conditions. However, the strength of self-doping of sulfonated polyanilines like PMAS (Figure 1b)[3] allows them to resist bases to an extent, providing for high conductivity up to a pH of 12.[4] Again, improving on this impressive function would further open the class up for practical application.

As an example of conformational control in PMAS, Kane-Maguire and co-workers shifted PMAS conformation from extended to compact coil by increasing pH.[5] Meanwhile, Hirao and co-workers have reported the redox-induced reversible conformational switching of PMAS.[6]

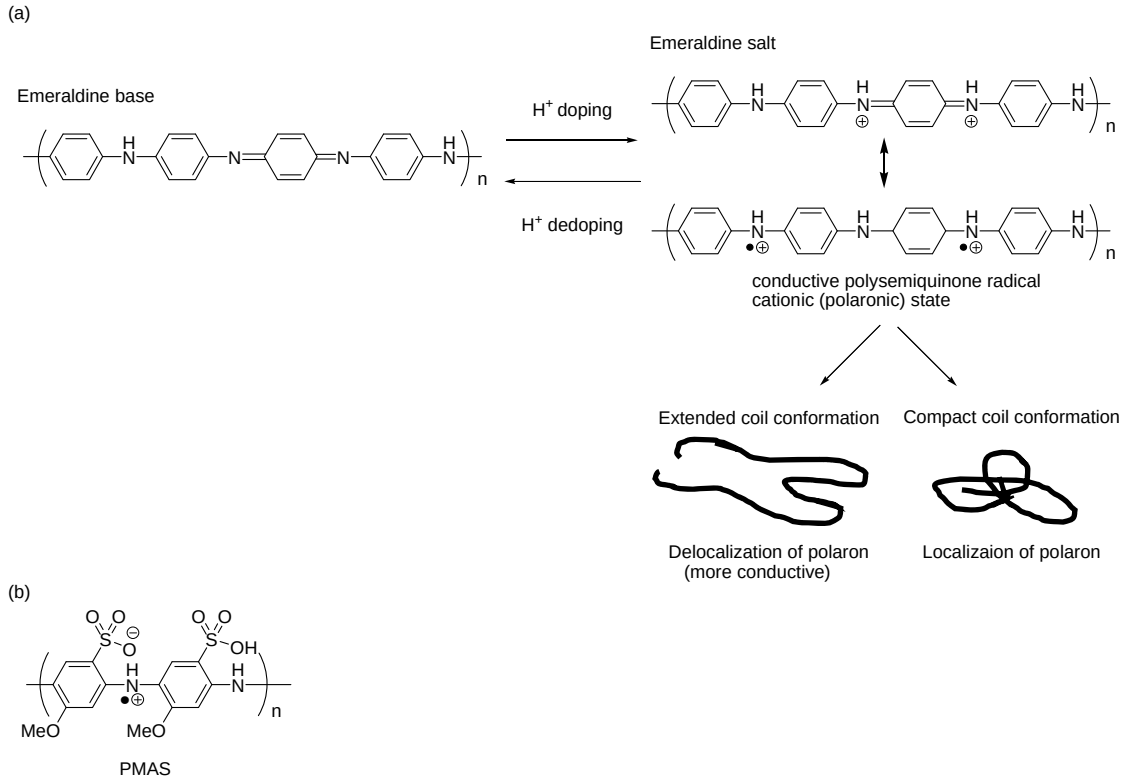

Figure 1. (a) Doping of polyaniline (emeraldine base). (b) Structure of PMAS.

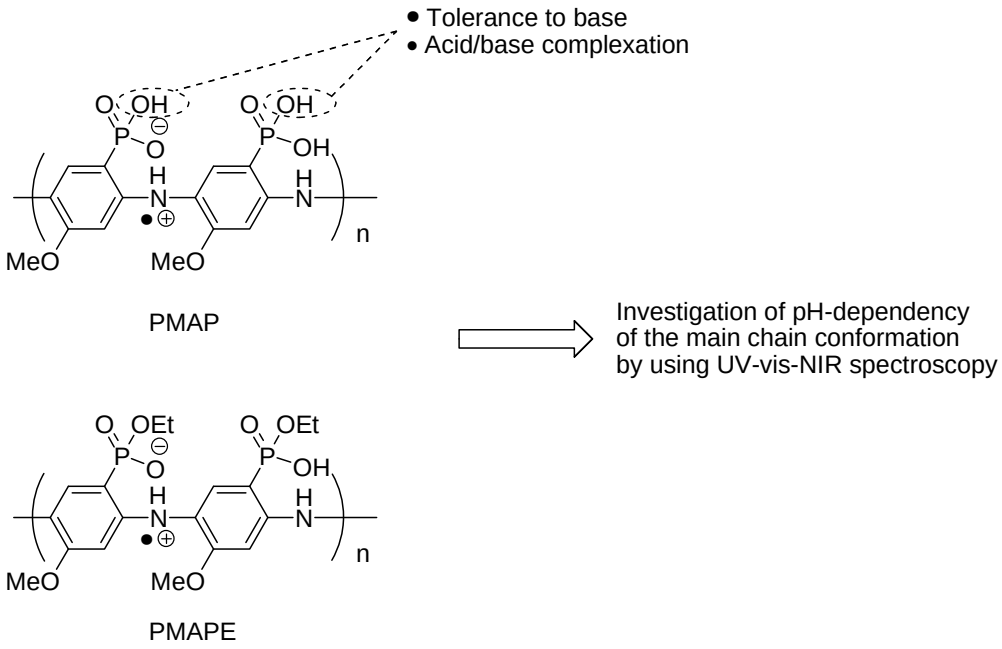

Figure 2. Structures of PMAP and PMAPE, and this work in chapter 5.

While the first phosphonic acid proton in PMAP is likely utilized in doping, the second one should, in theory, improve base tolerance and allow for salt formation through acid/base complexation, which would in turn affect the conformation of the main chain. These conformational changes are reflected in the UV-vis-NIR absorption spectra.[1] Specifically, the polaron band (around 440 nm) and localized polaron band (around 780 nm) diagnostic peaks correspond to the extended and compact coil conformations, respectively.[1] A stedily increasing free carrier tail starting at about 1000 nm can also be used as a diagnosis for metallic conductive materials because such free carrier tail arises from the delocalization of electrons in the polaron band that are promoted by a straightening of the polymer main chain in the extended coil.[1,7] This chapter uses this information to assess the pH-dependency of PMAP and PMAPE conformation and electron delocalization (Figure 2).

5-2. Results and discussion

UV-vis-NIR spectroscopy was used to track spectral changes to an acidic PMAP solution that was slowly increased in pH using 1 M aqueous NaOH. Figures 3a and 3b show the corresponding spectra for a PMAP/pyridine complex at a 1:1 ratio with respect to the aniline unit. Here, pyridine was added to improve solubility because PMAP by itself is not soluble in water.

PMAP was present in the extended coil conformation at pH 5.95, as indicated by the polaron band (around 440 nm) and free carrier tail (>1000 nm) in the spectra (Figure 3a). At this pH, the solution

was brown. Between pH values of 5.95 to 8.98, the polaron band decreased in intensity while the free carrier tail increased, an effect that continued even slightly beyond this range; at the same time, the color changed from brown to green. Likewise, the peak at around 700 nm, which is presumably the localized polaron band, appeared as the pH became more basic. These effects could result from partial conformational change, an effect that has been previously reported for PMAS.[5] In addition, an increase in the free carrier tail intensity is not usual in conducting polyanilines, as de-doping normally occurs at increasing pH values.[8] In contrast, the free carrier tail decreases monotonically for PMAS as pH values increase due to this conformational change, yet in this case, the self-doping of the material prevents de-doping from occurring.[5]

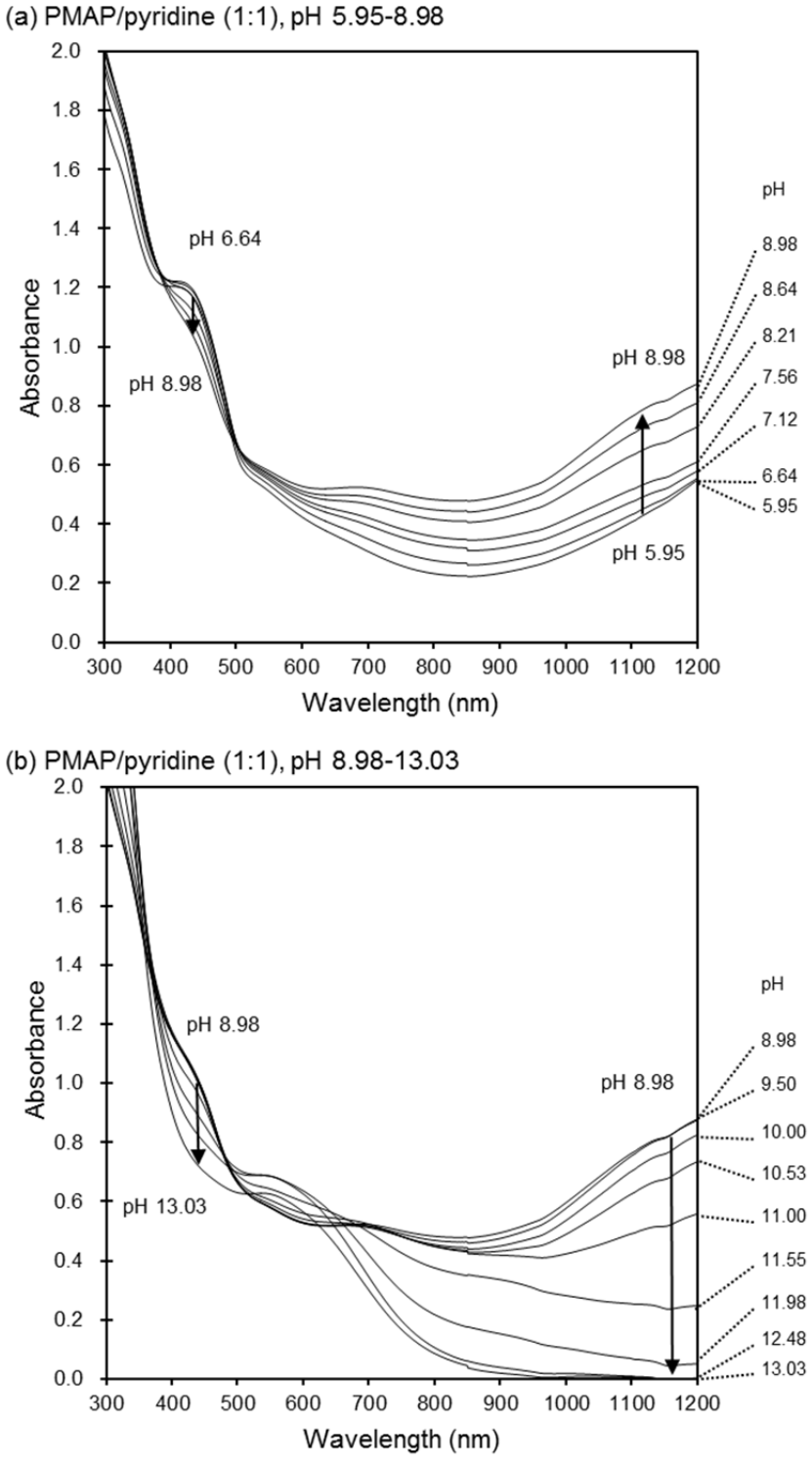

Figure 3. UV-vis-NIR spectra of PMAP/pyridine (1:1) (4.9×10^{-4} M aqueous solution) in a range of (a) pH 5.95 to 8.98 and (b) pH 8.98 to 13.03, and PMAP (4.9×10^{-4} M aqueous solution) in a range of (c) pH 7.12 to 10.02 and (d) pH 10.02 to 12.97. Concentration is calculated based on the aniline unit.

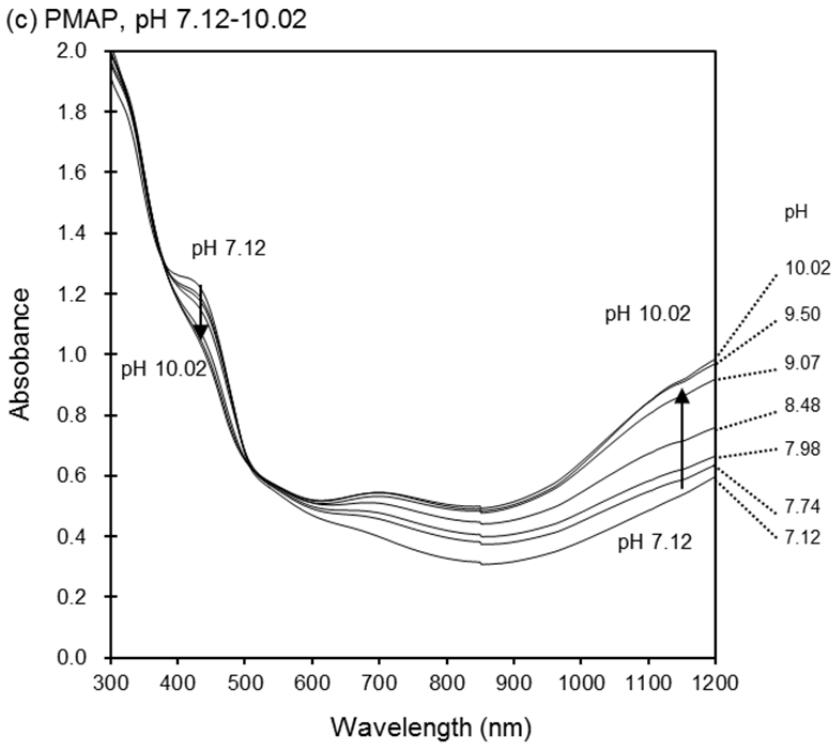
(c) PMAP, pH 7.12-10.02
Absobance
Wavelength (nm)
pH 7.12
pH 10.02
pH 10.02
pH 7.12
pH
10.02
9.50
9.07
8.48
7.98
7.74
7.12

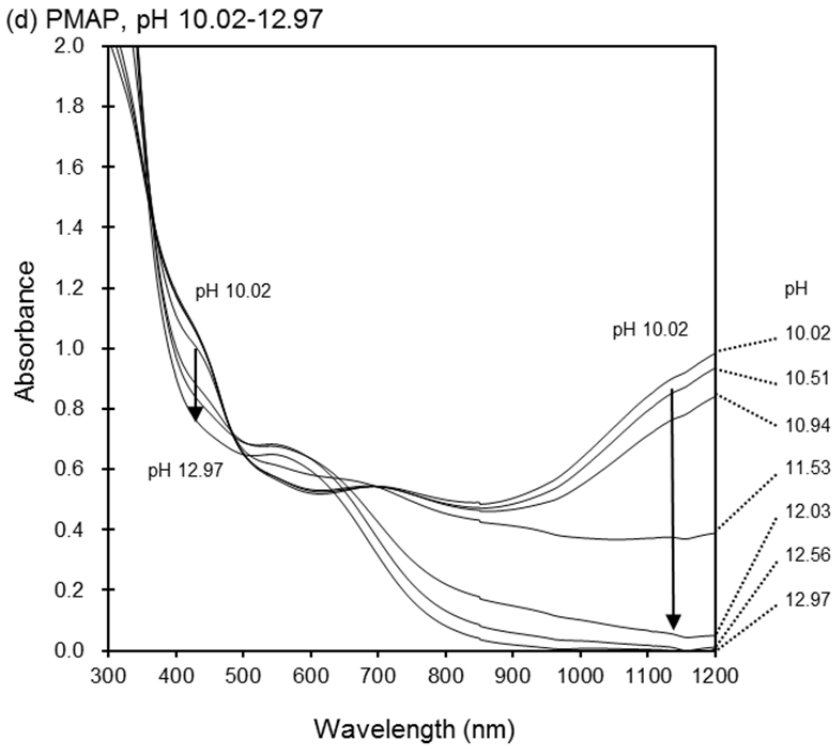
(d) PMAP, pH 10.02-12.97
Absorbance
Wavelength (nm)
pH 10.02
pH 12.97
pH 10.02
pH
10.02
10.51
10.94
11.53
12.03
12.56
12.97

These uncharacteristic effects might result from the straightening of the polyaniline main chain, which in turn could be due to electrostatic repulsion between the negatively charged phosphonate anions that are not involved in doping (Figure 4).

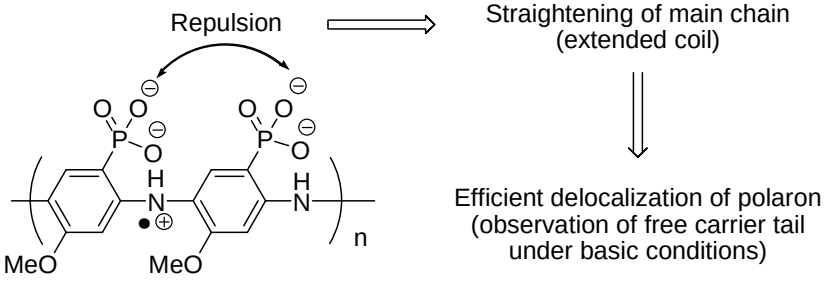

Figure 4. Proposal for the mechanism of efficient delocalization of polaron under basic conditions.

Previous work by Chan et al. in which the phosphate moiety was attached to the polyaniline main chain by a methylene bridge included an absorption spectra of the sodium salts, as well as the retention of a slight polaronic character.[9] However, the spectra taken did not include the NIR region, while the behavior of the free carrier tail observed herein was not described. This effect began to reverse in the PMAP case at a pH of around 9.50, though intensity was high even until a pH of 10.5 and was still at about 60% of the maximum intensity at 1200 nm by a pH of 11 (Figure 3b). Meanwhile, the polaron band at around 430 nm also decreased between pH values of 8.98 to 13.03. At the same time, a broad peak at around 550 nm appeared, while the peak at around 700 nm disappeared. The former peak is attributed to the benzenoid-to-quinoid CT transition in the main chain,[4,10] indicating dedoping. Note that the color of the solution changed from green to purple in this range.

To investigate the effect of pyridine, similar experiments were conducted without it. Due to the low acidic solubility of PMAP, these experiments were limited to a pH range of 7.12 to 12.97. Overall, though, similar spectral change was observed (Figures 3c and 3d). For example, the free carrier tail continued to increase until a pH of 10.02, and was still fairly intense until a pH of about 11. This indicated that base resistance improved slightly in the absence of pyridine.

The pH dependence of electrical conductivity was also investigated, this time using drop-cast films of PMAP/pyridine (at a 1:1 ratio with respect to the aniline unit). The film formed at a pH of 5.61 in aqueous solution showed a conductivity of 9 S/m. However, increasing the basicity above a pH of 7.32 decreased conductivity to the point where it could no longer be detected. This could be explained by a decrease in carriers (consistent with the decreasing intensity of the polaron band at around 430 nm, as show in Figure 1) and/or by inefficient carrier hopping between chains in the bulk conditions.

Figure 5a shows the variable pH UV-vis-NIR spectra for the PMAPE/pyridine complex (at a 1:0.5 ratio with respect to the aniline unit) over a pH range of 6.20 to 13.00. The observed changes were simple, in sharp contrast to those in the PMAP/pyridine analysis. PMAPE was present in the extended coil conformation at a pH of 6.20, as demonstrated by the presence of the polaron band and free carrier tail at around 450 nm and above 1000 nm, respectively. Both of these regions decreased in intensity as the pH became more basic. At the same time, the broad peak at 710 nm presumably representing the localized polaron band appeared and slightly increased in intensity until a pH of 8.13. At this point, the CT band peak at about 600 nm increased as well. The final spectrum, taken at a pH of 13.00, is typical for emeraldine bases of polyaniline.[4,10] This suggests the de-doping of PMAPE via compact coil conformation. In addition, the color of the solution changed from greenish brown (pH ~6.0) to green (pH ~9.0), and finally to blue-purple (pH ~13.0).

As before, the effect of pyridine was also investigated at a pH range of 7.07 to 12.94. Nearly identical changes were observed (Figure 5b), suggesting that pyridine plays little effect under these conditions.

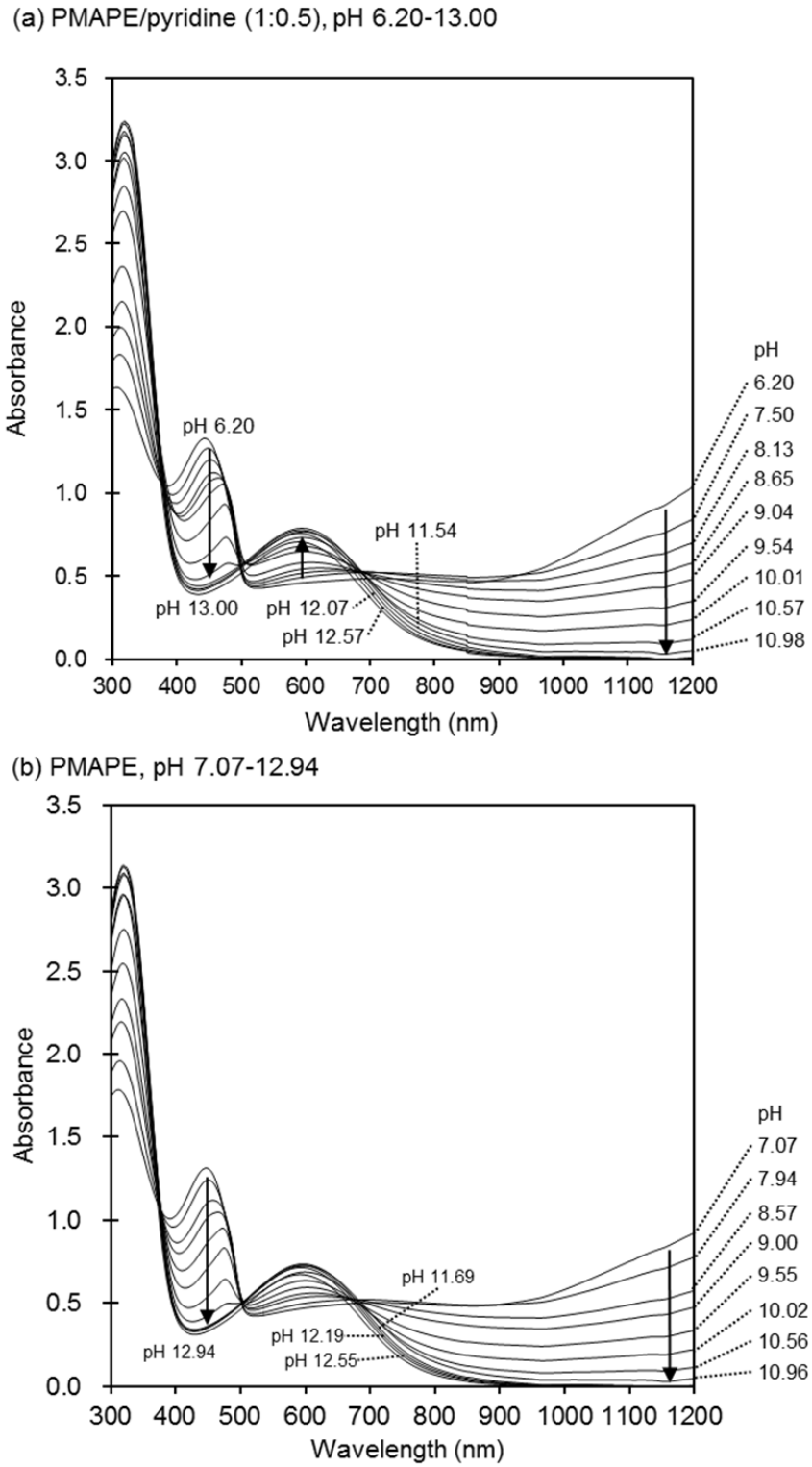

Figure 5. UV-vis-NIR spectra of PMAPE/pyridine (1:0.5) (4.4 x 10^{-4} M aqueous solution) in a range of (a) pH 6.20 to 13.00, and PMAPE (4.4 x 10^{-4} M aqueous solution) in a range of (b) pH 7.07 to 12.94. Concentration is calculated based on the aniline unit.

In conclusion, PMAP exhibits efficient deprotonation-induced polaron delocalization, as suggested by pH-dependent investigations of PMAP and PMAPE using UV-vis-NIR spectroscopy. For example, the free carrier tail of PMAP increases with pH, up to about 9.50. This is extraordinary because dedoping normally occurs as pH increases. In contrast, PMAPE exhibited the expected spectral change, including the monotonic decrease of polaron band and free carrier tail intensity as pH increased. These contrasting results seem to result from the difference in the number of protons. The anionic repulsion that seemingly results in the case of PMAP may induce an even greater straightening of the polyaniline main chain under basic conditions.

5-3. Experimental

General

Preparation of PMAP and PMAPE were described in chapter 1-3. Milli-Q water was used in the experiments using UV-vis-NIR absorption spectroscopy. UV-vis-NIR absorption spectra were recorded on a JASCO V-670 spectrometer. pH of solutions was recorded on a HORIBA D-51 pH meter. Electrical conductivity measurements were performed by using the same method of chapter 1. The measurements of the electrical resistance for a two-probe method were conducted using a circuit tester (CUSTOM, CX-180N) under environmental conditions.

Variable pH UV-vis-NIR absorption spectral experiments

PMAP (9.96 mg, 0.049 mmol for the experiment in Figures 3a and 3b, 10.10 mg, 0.049 mmol for the experiment in Figures 3c and 3d) or PMAPE (10.02 mg, 0.044 mmol for the experiment in Figure 5a, 10.10 mg, 0.044 mmol for the experiment in Figure 5b), and 1 M aqueous pyridine solution (49 μL, 0.049 mmol for the experiments in Figures 3a and 3b, 22 μL, 0.022 mmol for the experiment in Figure 5a) were diluted with water in measuring flask to 100 mL total. The solution was transferred into a beaker with a stirrer bar. A pH meter was immersed in the solution. To the stirred solution, 1 M aqueous NaOH solution (ca. 15 μL) was added until the acidity of the solution became around pH 6.0 for the experiments in Figures 3a, 3b, and 5a, and around pH 7.0 for the experiments in Figures 3c, 3d, and 5b. Approximately 3 mL of the solution was transferred to a cuvette (1 cm path length), and the absorption spectrum of the solution was measured at 25 °C. The solution in the cuvette was returned to the beaker. Then, 1 M aqueous NaOH solution was added, and the absorption spectrum of the solution was again measured at 25 °C. This sequence was repeated until around pH 13 in increments of about 0.5. After pH 12, amounts of the added 1 M aqueous NaOH solution were several mL, therefore the effect of the dilution with 1 M aqueous NaOH solution is relatively large in a range of pH 12 to 13.

5-4. References and notes

1. Y. Xia, J. M. Wiesinger, A. G. MacDiarmid, *Chem. Mater.* **1995**, *7*, 443-445.
2. J. Yue, A. J. Epstein, *J. Am. Chem. Soc.* **1990**, *112*, 2800-2801.
3. S. Shimizu, T. Saitoh, M. Uzawa, M. Yuasa, K. Yano, T. Maruyama, K. Watanabe, *Synth. Met.* **1997**, *85*, 1337-1338.
4. X.-L. Wei, Y. Z. Wang, S. M. Long, C. Bobeczko, A. J. Epstein, *J. Am. Chem. Soc.* **1996**, *118*, 2545-2555.
5. E. V. Strounina, R. Shepherd, L. A. P. Kane-Maguire, G. G. Wallace, *Synth. Met.* **2003**, *135-136*, 289-290.
6. T. Amaya, D. Saio, S. Koga, T. Hirao, *Macromolecules* **2010**, *43*, 1175-1177.
7. A. G. MacDiarmid, A. J. Epstein, *Synth. Met.* **1994**, *65*, 103-116.
8. A. G. MacDiarmid, *Angew. Chem. Int. Ed.* **2001**, *40*, 2581-2590.
9. H. S. O. Chan, P. K. H. Ho, S. C. Ng, B. T. G. Tan, K. L. Tan, *J. Am. Chem. Soc.* **1995**, *117*, 8517-8523.
10. L. L. Premvardhan, S. Wachsmann-Hogiu, L. A. Peteanu, D. J. Yaron, P.-C. Wang, W. Wang, A. G. MacDiarmid, *J. Chem. Phys.* **2001**, *115*, 4359-4366.

Chapter 6. Evaluation of the charge dissipation properties of PMAP/amine complexes in electron beam lithography[P6]

6-1. Introduction

Self-doped conducting polymers are attractive materials not only because of their conductivity, but also due to their water processability, leading to a wide range of applications in biosensors and electronic materials.[1] Charge dissipation is an important feature in electron beam (e-beam) lithography because charging of the resist and substrate during exposure can deflects the electron beam path, resulting in image distortion and pattern placement error. Coating of the resist with conducting polymers has proven to be an effective means of avoiding this problem.[2] Water soluble conducting polymers are especially suitable for this purpose because they can be selectively removed by washing with aqueous solution without dissolving the hydrophobic resist. Poly(isothianaphthenediylsulfonate) and poly(thienylalkanesulfonate), self-doped conducting polymers, are particularly effective,[2] to the extent that they are currently in commercial use.[3] In recognition of the similarities between these polymers and those developed herein, this chapter describes the conductivity of the various amine complexes of PMAP and PMAPE and assesses the charge dissipation properties of some specific PMAP/amine complexes.

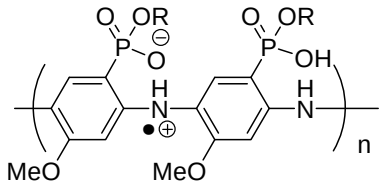

PMAP : R = H, PMAPE : R = Et

Figure 1. Structures of PMAP and PMAPE.

6-2. Results and discussion

6-2-1 *Electrical conductivity*

The electrical resistance of the drop-cast polyaniline/amine films was measured by the DC method used in chapter 1. The complexes were prepared by mixing them in water to obtain 1% (w/w, based on the amount of PMAP or PMAPE) solutions or suspensions, with a variable amount of amine in each case that was measured with respect to the repeat aniline unit in the polyaniline.

Table 1 summarizes the electrical resistance and conductivity of the PMAP/amine complexes. In the case of the pyridine, $CF_3CH_2NH_2$, NH_3, and NEt_3 complexes, one molar equivalent of amine did not yield a homogenous solution, but a suspension (Table 1, entries 1, 4, 7, and 10). The pyridine

and $CF_3CH_2NH_2$ complexes exhibited conductivity in a range of 9-19 S/m (Table 1, entries 1-6); these values did not decrease significantly even in the presence of four equivalents of the amine. The weight of the PMAP/pyridine (1:2 and 1:4) complexes was measured by TGA after drying at 100 °C for 10 min. If all of the phosphonic acid moieties in the PMAP formed complexes with pyridine, the theoretical weight increase should equal 178%; however, the observed weight increase was 116 and 111% for the PMAP/pyridine (1:2 and 1:4) complexes, respectively, suggesting that only 21 and 14 mol% of the phosphonic acid hydroxyl groups underwent complexation, respectively. This may explain why amine amount played little effect on conductivity.

The conductivity of the NH_3 and 4-pyridinemethanol complexes was almost one order of magnitude smaller than the previously mentioned ones (0.5-3 S/m; Table 1, entries 7-9 and 21). Combinations of amines, such as pyridine and NEt_3 and $CF_3CH_2NH_2$ and NEt_3, exhibited almost the average values for the two constituents (Table 1, entries 13-16). Meanwhile, the NEt_3, diethanolamine, methyl diethanolamine, and *N*,*N*′-dimethyl-4-aminopyridine (DMAP) complexes showed electrical resistances that were too large to allow for an estimation of conductivity. Overall, the data suggest that conductivity decreases as amine basicity increases (the pKa of the protonated forms of the following amines are: pyridine 5.21, NH_3 9.2, NEt_3 10.75, imidazole 6.95, DMAP 9.2).[4] In fact, strong amines seem to inhibit the acid doping process even if just one equivalent (with respect to one phosphonic acid moieties) is used.

Table 1. Electrical resistance and conductivity for the drop-cast films of the aqueous 1% (w/w)[a] suspension/solution of the amine complexes of PMAP.

Entry	Amine	Molar equivalents of amine[b]	Suspension or solution	Electrical resistance (kΩ)	Conductivity (S/m)[c]
1	Pyridine	1	Suspension	14	19[d]
2	Pyridine	2	Solution	20	13[d]
3	Pyridine	4	Solution	20	13[d]
4	$CF_3CH_2NH_2$	1	Suspension	30	9
5	$CF_3CH_2NH_2$	2	Solution	20	13
6	$CF_3CH_2NH_2$	4	Solution	20	13
7	NH_3	1	Suspension	500	0.5
8	NH_3	2	Solution	500	0.5
9	NH_3	4	Solution	100	3
10	NEt_3	1	Suspension	>1000	–
11	NEt_3	2	Solution	>1000	–
12	NEt_3	4	Solution	>1000	–
13	Pyridine/NH_3 (4:1)	2	Solution	25	11
14	Pyridine/NH_3 (1:1)	2	Solution	400	0.7
15	$CF_3CH_2NH_2$/NH_3 (4:1)	3	Solution	50	5
16	$CF_3CH_2NH_2$/NH_3 (1:1)	2	Solution	300	0.9
17	Diethanolamine	2	Solution	>1000	–
18	Methyl diethanolamine	2	Solution	>1000	–
19	Imidazole	1	Solution	>1000	–
20	N,N'-Dimethyl-4-aminopyridine	1	Solution	>1000	–
21	4-Pyridinemethanol	1	Solution	400	0.7

[a] Based on the amount of PMAP.
[b] Based on the aniline unit.
[c] Conductivity was calculated on the assumption that the gap was filled with the polymer. Therefore, the obtained value is the minimum value.
[d] Values of chapter 1.

Thermal stability of the PMAP/pyridine (1:2) complex was investigated by TGA (Figure 2). A sharp weight loss was observed at approximately 170-230 °C, an effect that is not observed for PMAP in isolation. Above this range, the slopes of the two are very similar. As such, this initial effect is likely the result of the loss of pyridine.

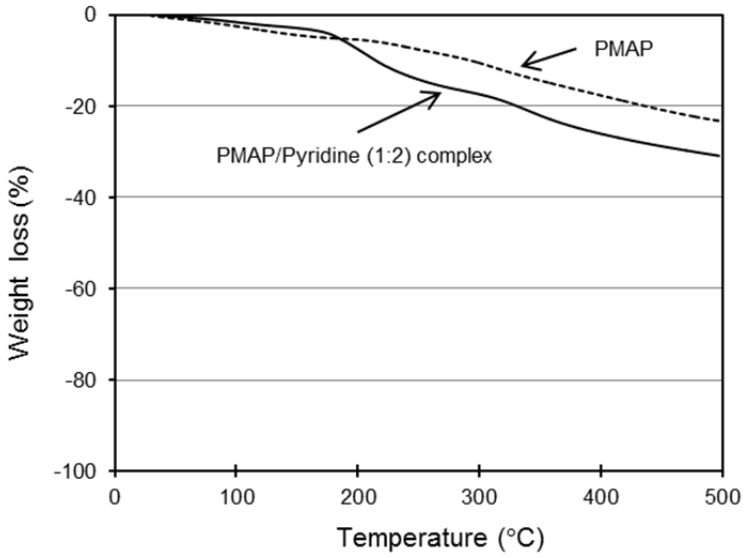

Figure 2. TGA curves for PMAP (dotted line) and PMAP/pyridine (1:2) complex (solid line) under a nitrogen atmosphere. The line of PMAP was adopted from chapter 4.

Table 2. Electrical resistance and conductivity for the drop-cast films of the aqueous 1% (w/w)[a] suspension/solution of complexes of PMAPE.

Entry	Amine	Molar equivalents of amine[b]	Suspension or solution	Electrical resistance (kΩ)	Conductivity (S/m)[c]
1	Pyridine	1	Solution	200	1[d]
2	Pyridine	2	Solution	200	1[d]
3	$CF_3CH_2NH_2$	1	Solution	100	3
4	$CF_3CH_2NH_2$	2	Solution	100	3
5	NH_3	1	Solution	500	0.5
6	NH_3	2	Solution	600	0.4
7	NEt_3	1	Solution	>1000	–
8	NEt_3	2	Solution	>1000	–

[a] Based on the amount of PMAPE.
[b] Based on the aniline unit.
[c] Conductivity was calculated on the assumption that the gap was filled with the polymer. Therefore, the obtained value is the minimum value.
[d] Values of chapter 3.

Table 2 summarizes the electrical resistance and conductivity data for the PMAPE/amine complexes. The conductivity values for most of the complexes are smaller than the corresponding PMAP samples, although the relationship between conductivity and basicity seems to hold.

6-2-2 *Charge dissipation properties*

The charge dissipation properties of PMAP/pyridine (1:2) were qualitatively evaluated by patterning a resist on a quartz substrate. The pattern shown in Figure 4a was designed so that the effect of increasing charge in the square (100 μm x 100 μm, exposed with 300 $\mu C/cm^2$) can be observed as a distortion in the lines (10 of a100 x 1 μm lines with 1 μm interspaces, exposed with 140 $\mu C/cm^2$). Either PMAP/pyridine (1:2) or Espacer 300Z, a commercially available charge dissipation agent,[3] was top-coated on a resist by spin-coating. The PMAP/pyridine (1:2) film was 25 nm in thickness. The development of top coating materials was employed with an aqueous NMe_4OH solution.

Figures 3b and c show photographs of the resist patterns for samples top coated with the PMAP/pyridine complex and Espacer 300Z, respectively, while Figure 3d shows the resist pattern for a sample without top-coating. The PMAP sample showed no image distortion or pattern placement error, a result that is comparable to that obtained for the Espacer 300Z. However, significant line distortion was observed when no charge dissipation layer was used, clearly demonstrating that the PMAP sample prevented charge accumulation.

Excess exposure was observed near the center of several lines close to the square for both charge dissipation trials. This is called the proximity effect, and is caused by electron backscattering from the substrate. Because the purpose of this study is only the evaluation of the charge dissipation properties of the PMAP complexes, no correction was attempted in the exposure design. The reason why the proximity effect was not observed in the sample without a charge dissipation layer is unclear. It is possible, though, that the exposure dose near the center of the boundary between the square and line patterns was reduced through the deflection of incident and backscattered electrons by the charge accumulation.

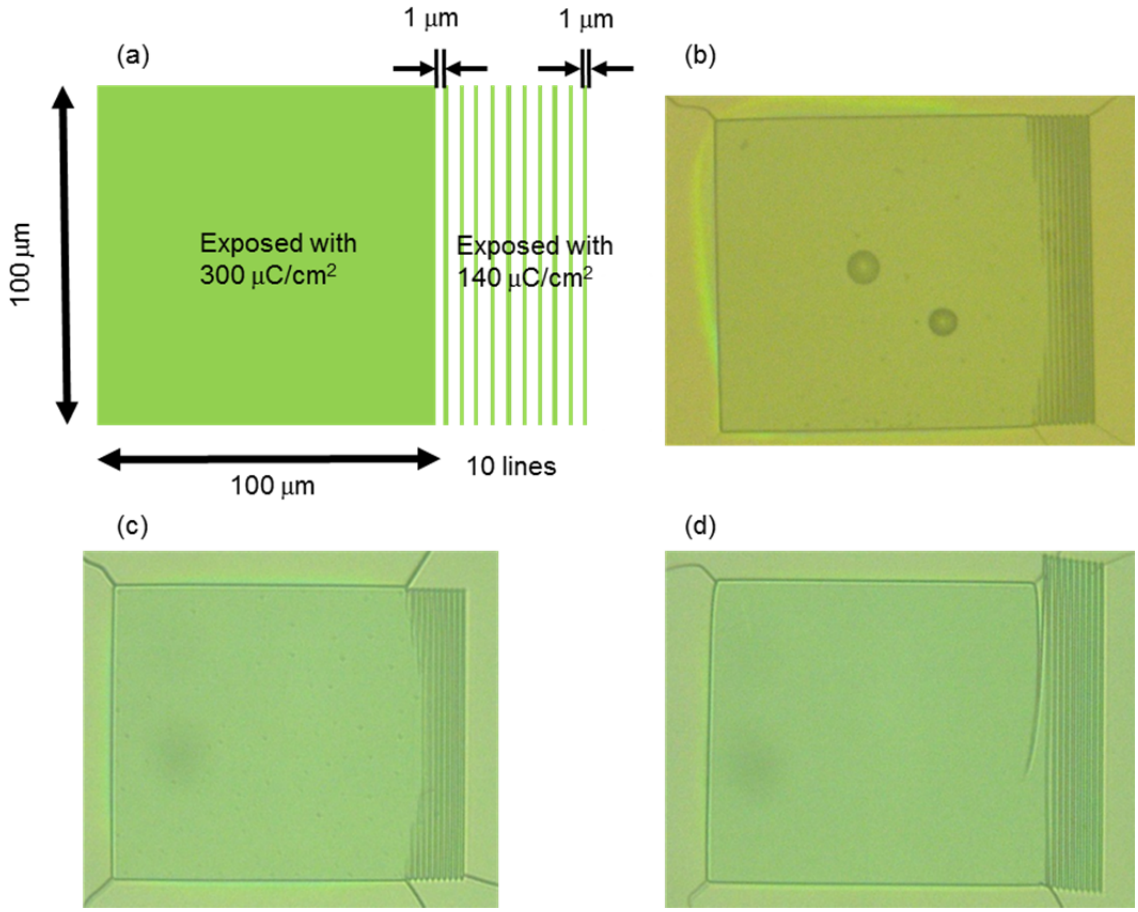

Figure 3. The resist patterning in the e-beam lithography. (a) Schematic image for the patterning, and the photographs using the charge dissipation film of (b) the PMAP/pyridine (1:2) complex, (c) Espacer 300Z, and (d) none, respectively, where the development was carried out with an aqueous NMe_4OH solution.

Aqueous NMe_4OH was used as the development solution for the PMAP/pyridine (1:2) complex. On the other hand, the use of water gives an advantage in the practical development process. Therefore, other complexes were investigated with the aim of finding a top-coat layer that could still be washed away with water. While the PMAP/$CF_3CH_2NH_2$ (1:4) complex exhibited good film-forming properties, it left some residual solids after washing. On the other hand, the PMAP/pyridine-4-ethanol (1:2) complex exhibited slightly worse film-forming properties but could more easily be washed away. This trend was even more exacerbated with the PMAP/NH_3 (1:2) complex.

Unfortunately, no one material was found that optimized both properties; as such, mixed amine complexes (shown in Table 1, entries 13-16) were investigated next, and all showed improved performance in both regards. Out of all of these, the PMAP/{$CF_3CH_2NH_2$/NH_3 (4: 1)} (1:3) was

investigated in detail. A photograph of the resist pattern is provided in Figure 4, and demonstrates good performance given the lack of line distortion. In addition, while the performance is comparable to that obtained with the PMAP/pyridine (1:2) complex and aqueous NMe_4OH development solution, this mixed complex was sufficiently soluble in water to be washed away effectively.

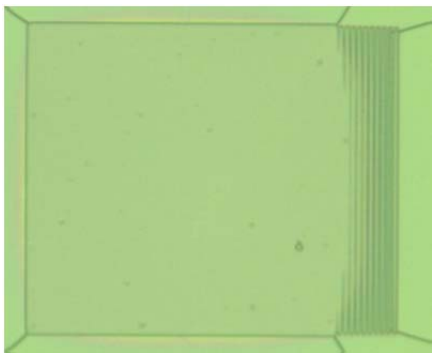

Figure 4. The resist patterning in the e-beam lithography using the charge dissipation film of the PMAP/{$CF_3CH_2NH_2$/NH_3 (4:1)} (1:3) complex, where the development was carried out with water.

In conclusion, the conductivity of drop-cast films for various amine complexes of PMAP and PMAPE was shown to be dependent on the basicity and quantity of the amine used. PMAP and PMAPE showed similar trends in behavior, yet PMAP demonstrated higher conductivity overall. In the case of the pyridine and $CF_3CH_2NH_2$ complexes of PMAP, conductivities of more than 10 S/m were retained even when four equivalents of the amine (with respect to the phosphonic acid moiety) were used. The charge dissipation properties for e-beam lithography of the PMAP/pyridine (1:2) complex was also investigated qualitatively by top-coating a resist on a quartz substrate. The obtained pattern clearly exhibited performance that was comparable to the commercially available charge dissipation agent Espacer 300Z. Meanwhile, the PMAP/{$CF_3CH_2NH_2$/NH_3 (4:1)} (1:3) complex showed similar performance while not requiring the use of NMe_4OH to aid in solubility. The practical application is expected as a charge dissipation agent in e-beam lithography.

6-3. Experimental

General

PMAP and PMAPE were prepared according to the procedures of chapter 1-3. The *Mw* of PMAP and PMAPE are 2.0 x 10^3 and 4.3 x 10^3, respectively (chapters 1 and 3). Other reagents were purchased from commercial sources. Milli-Q water was used to prepare the aqueous solution. Electrical conductivity measurements were performed by the same method of chapter 1. The measurements of the electrical resistance for a two-probe method were conducted using a circuit tester (CUSTOM, CX-180N) under environmental conditions.

Preparation of the amine complexes

The aqueous solution of amine was added to the aqueous solution of PMAP or PMAPE, where the total concentration was controlled to be 1% w/w based on the amount of PMAP or PMAPE.

TGA

TGA was recorded on a SII TG/DTA6200 analyzer. Samples were put in open aluminum pan and measured under a nitrogen atmosphere (flow rate 150 mL/min).

Charge dissipation agent measurements

A main-chain scission-type positive-tone resist, ZEP 520A (copolymer of α-chloromethacrylate and α-methylstyrene, ZEON) was used as a resist material. ZEP 520A resist solution was spin-coated onto quartz substrates at 3000 rpm for 30 s. The spin-coated films were prebaked for 10 min at 180 °C. In order to investigate whether the charge-up was prevented or not using top-coating materials, we investigated the line distortion in designed patterns with and without top-coating materials. In the case of using top-coating, conducting polymers such as PMAP/pyridine (1:1), PMAP/{($CF_3CH_2NH_2$/NH_3 (4:1)} (1:3) or Espacer 300Z were spin-coated at 2000 rpm for 60 s before exposure. Then, the ZEP 520A films with and without top-coating were exposed to a 75 kV e-beam (ELIONIX, ELS-7700). The irradiated area consisted of two parts. One is a big square pattern, (100 μm × 100 μm) (Figure 4a), which was exposed at a dose of 300 μC/cm^2. The other is a small pattern, which is composed of 10 lines and 10 spaces (Figure 4a). The line width and length are 1 μm and 100 μm, respectively. They were exposed at a dose of 140 μC/cm^2. Top-coating materials were developed by dipping in NMD-3 (NMe_4OH, Tokyo Ohka Kogyo) solutions for the case of using PMAP/pyridine (1:1) and Espacer 300Z, or deionized water for the case of using PMAP/{($CF_3CH_2NH_2$/NH_3 (4:1)} (1:3), at 23 °C for 30 s and then rinsed in deionized water before drying. Subsequently, the resist was developed in ZMD-N50 (*n*-amyl acetate, ZEON) developer for 60 s and rinsed with ZMD-B (89:11 methyl isobutyl ketone/isopropyl alcohol w/w, ZEON), which is

a rinse solution. The photographs of resist patterns were recorded with a digital microscope (KEYENCE, VHX-200).

6-4. References and notes

1. M. S. Freund, B. Deore, Self-Doped Conducting Polymers, John Wiley & Sons, Ltd., New York, 2007.
2. H. Tomozawa, Y. Saida, Y. Ikenoue, F. Murai, Y. Suzuki, T. Tawa, Y. Ohta, *J. Photopolym. Sci. Technol.* **1996**, *9*, 707-714.
3. Commercially available as Espacer from Showa Denko http://www.showadenko.us/product/espacer.html. Espacer 300Z is a charge dissipation agent for a chemical amplified and positive resist among Espacers.
4. From Evance pKa Table: http://evans.rc.fas.harvard.edu/pdf/evans pKa table. pdf.

Conclusion

In this dissertation, novel self-doped conducting polyanilines bearing phosphonic acid (PMAP) and phosphonic acid monoester (PMAPE) moieties were successfully synthesized. These are the first examples of direct attachment of this class of functionality to a polyaniline backbone. The results obtained from investigating the properties of these materials are therefore important in that they contribute directly to the continued development of the field of conducting polymers.

In chapter 1, PMAP was synthesized, and its self-doping and conductivity characteristics were clearly demonstrated.

In chapter 2, a practical synthesis of PMAP was developed.

In chapter 3, PMAPE was synthesized, and its self-doping and conductivity characteristics were reviewed.

In chapter 4, the thermostability, solid-state morphology, spin-coated film absorption and transparency, polaron delocalization, doping efficiency, and chemical oxidative and reductive properties of PMAP and PMAPE were investigated.

In chapter 5, the pH-dependent behavior of PMAP and PMAPE in solution was investigated. In the case of PMAP, deprotonation of the phosphonic acid moiety induced efficient polaron delocalization.

In chapter 6, the conductivity of the various amine complexes of PMAP and PMAPE was investigated. The PMAP/pyridine (1:2) and PMAP/{$CF_3CH_2NH_2/NH_3$ (4:1)} (1:3) complexes in particular exhibited charge dissipation properties.

The author expects that PMAP and PMAPE will be used as conducting materials, charge dissipation agents, redox mediators, and synthetic metal catalysts, among others, in the near future.

List of publications

P1. "Synthesis of self-doped conducting polyaniline bearing phosphonic acid"
Toru Amaya, Yasushi Abe, Yuhi Inada, and Toshikazu Hirao
Tetrahedron Lett. **2014**, *55*, 3976-3978.

P2. "Practical synthesis of poly(2-methoxyaniline-5-phosphonic acid), a self-doped conducting polyaniline bearing phosphonic acid"
Yasushi Abe, Toru Amaya, and Toshikazu Hirao
Bull. Chem. Soc. Jpn. **2014**, *87*, 1026-1028.

P3. "Synthesis of self-doped conducting polyaniline bearing phosphonic acid monoester"
Toru Amaya, Yasushi Abe, Yuhi Inada, and Toshikazu Hirao
Synth. Met. **2014**, *195*, 137-140.

P4. "Characterization of self-doped conducting polyanilines bearing phosphonic acid and phosphonic acid monoester"
Yasushi Abe, Toru Amaya, Yuhi Inada, and Toshikazu Hirao
Synth. Met. **2014**, *197*, 240-245.

P5. "Deprotonation-induced efficient delocalization of polaron in self-doped poly(anilinephosphonic acid)"
Toru Amaya, Yasushi Abe, and Toshikazu Hirao
Macromolecules **2014**, *47*, 8115-8118.

P6. "Conductivity of poly(2-methoxyaniline-5-phosphonic acid)/amine complex and its charge dissipation property in electron beam lithography"
Toru Amaya, Yasushi Abe, Hiroki Yamamoto, Takahiro Kozawa, and Toshikazu Hirao
Synth. Met. **2014**, *198*, 88-92.

List of patent

1. "Method for producing polyaniline having self-doping function and antistatic agent containing polyaniline produced thereby"
Toshikazu Hirao, Toru Amaya, and Yasushi Abe
Application number：2013-84037 (Japan), PCT/JP2014/001971 (PCT), 103113492 (Taiwan).

List of supplementary publications

S1. "Crystal structure of *anti*-1,4,5,8-tetrapropyl-1,4:5,8-diepoxyanthracene"
Chitoshi Kitamura, Yasushi Abe, Mikio Ouchi, and Akio Yoneda
Anal. Sci. **2004**, *20*, x27-x28.

S2. "Influence of alkyl chain length on the solid-state packing and fluorescence of 1,4,5,8-tetra(alkyl)anthracenes"
Chitoshi Kitamura, Yasushi Abe, Nobuhiro Kawatsuki, Akio Yoneda, Kohei Asada, Takashi Kobayashi, and Hiroyoshi Naito
Mol. Cryst. Liq. Cryst. **2007**, *474*, 119-135.

S3. "Synthesis and crystallochromy of 1,4,7,10-tetraalkyltetracenes: tuning of solid-state optical properties of tetracenes by alkyl side-chain length"
Chitoshi Kitamura, Yasushi Abe, Takuya Ohara, Akio Yoneda, Takeshi Kawase, Takashi Kobayashi, Hiroyoshi Naito, and Toshiki Komatsu
Chem. Eur. J. **2010**, *16*, 890-898.

Acknowledgements

The author would like to express his appreciation sincerely to Professor Dr. Toshikazu Hirao, Department of Applied Chemistry, Graduate School of Engineering, Osaka University for giving the author a wonderful opportunity and his guidance.

The author would like to appreciate Professor Dr. Satoshi Minakata, Department of Applied Chemistry, Graduate School of Engineering, Osaka University for reviewing this thesis.

The author also would like to appreciate Professor Dr. Takahiro Kozawa, The Institute of Scientific and Industrial Research, Osaka University for reviewing this thesis and collaboration.

The author would like to express his gratitude deeply to Assistant Professor Dr. Toru Amaya, Department of Applied Chemistry, Graduate School of Engineering, Osaka University for his fruitful discussion and guidance.

The author would like to express his gratitude to Assistant Professor Dr. Hiroki Yamamoto, The Institute of Scientific and Industrial Research, Osaka University for the evaluation of charge dissipation properties of PMAP/amine complexes.

The author also would like to express his gratitude truly to Associate Professor Dr. Toshiyuki Moriuchi, Department of Applied Chemistry, Graduate School of Engineering, Osaka University for creating the better environment for the author to experiment in this study.

The author would like to thank Professor Dr. Shunichi Fukuzumi and Assistant Professor Dr. Tomoyoshi Suenobu, Department of Applied Chemistry, Graduate School of Engineering, Osaka University for the ESR measurements.

The author would like to thank Dr. Ryotaro Tsuji, Osaka University for the conductivity measurements by the four-point probe method.

The author would like to thank Comprehensive Analysis Center of the Institute of Scientific and Industrial Research, Osaka University for the ICP-MS measurements and SEM analysis.

The author would like to express his special thanks to Daihachi Chemical Industry and members of the company. Especially, the author would like to thank Mr. Yasuhiro Onishi (former director) deeply for giving the author an unforgettable opportunity to collaborate with Osaka University.

The author would like to thank all members of Hirao's group for helping him. Especially, the author would like to thank Mr. Yuhi Inada. Without his support, this thesis would not have been completed.

Finally, the author would like to appreciate so much the support from his wife, Keiko Abe, their sons, Sotaro Abe and Shinjiro Abe, and the author's parents, Mr. Nobuo Abe and Mrs. Hisako Abe.

Yasushi Abe